Available online at www.sciencedirect.com

ScienceDirect

International Journal of Solids and Structures 45 (2008) 276–302

INTERNATIONAL JOURNAL OF SOLIDS AND STRUCTURES

www.elsevier.com/locate/ijsolstr

Elastic waves in an electro-microelastic solid

S.K. Tomar *, Aarti Khurana

Department of Mathematics, Panjab University, Chandigarh 160 014, India

Received 8 November 2006; received in revised form 21 June 2007
Available online 6 September 2007

Abstract

The present study is concerned with the wave propagation in an electro-microelastic solid. The reflection phenomenon of plane elastic waves from a stress free plane boundary of an electro-microelastic solid half-space is studied. The condition and the range of frequency for the existence of elastic waves in an infinite electro-microelastic body are investigated. The constitutive relations and the field equations for an electro-microelastic solid are stemmed from the Eringen's theory of microstretch elasticity with electromagnetic interactions. Amplitude ratios and energy ratios of various reflected waves are presented when an elastic wave is made incident obliquely at the stress free plane boundary of an electro-microelastic solid half-space. It has been verified that there is no dissipation of energy at the boundary surface during reflection. Numerical computations are performed for a specific model to calculate the phase speeds, amplitude ratios and energy ratios, and the results obtained are depicted graphically. The effect of elastic parameter corresponding to micro-stretch is noticed on reflection coefficients, in particular. Results of Parfitt and Eringen [Parfitt, V.R., Eringen, A.C., 1969. Reflection of plane waves from a flat boundary of a micropolar elastic half-space. J. Acoust. Soc. Am. 45, 1258–1272] have also been reduced as a special case from the present formulation.

Keywords: Microstretch; Micropolar; Micro-rotation; Electro-microelastic; Electric; Amplitude; Energy; Reflection

1. Introduction

Eringen (1966) developed the linear theory of micropolar elasticity which is a subclass of the nonlinear theory of simple microelastic solids earlier developed by Eringen and his co-worker (1964a, b) and is a generalization of the classical theory of elasticity. The basic difference between the theory of micropolar elasticity and that of the classical theory of elasticity is the introduction of an independent microrotation vector. Thus, in the theory of micropolar elasticity, the motion in a body is characterized by six degrees of freedom, namely three of translation and three of rotation. The interaction between two parts of a micropolar body is transmitted not only by a force vector but also by a couple resulting in asymmetric force stress tensor and couple stress tensor. Many problems on wave propagation in micropolar elastic media have been investigated by several

* Corresponding author. Tel.: +91 172 2534523; fax: +91 172 2541132.
E-mail addresses: sktomar@yahoo.com (S.K. Tomar), aarti_maths@yahoo.com (A. Khurana).

0020-7683/$ - see front matter
doi:10.1016/j.ijsolstr.2007.08.014

researchers in the past, e.g., Smith (1967), Parfitt and Eringen (1969), Nowacki and Nowacki (1969), Ariman (1972), Tomar and Gogna (1995, 1997) and Tomar et al. (1998) among several others.

The linear theory of microstretch elastic solids developed by Eringen (1990) is a generalization of the theory of micropolar elasticity and is again a subclass of the theory of micromorphic materials. Microstretch elastic solids are those solids in which the material particles can undergo expansion and contraction (stretches), in addition to the translation and rotation. Thus the motion in a microstretch elastic body is characterized by seven degrees of freedom. The transmission of load across a differential element of the surface of a microstretch elastic solid is desribed by a force vector, a couple stress vector and a microstress vector. Composite materials reinforced with chopped elastic fibers and porous materials whose pores are filled with gas may fall in the category of microstretch elastic solids. Tomar and Garg (2005) investigated the possibility of wave propagation and discussed the reflection/transmission phenomena of plane waves at a plane interface between two different microstretch elastic solid half-spaces.

Later, Eringen (2004) extended his theory of microstretch elastic solids to include the electromagnetic interactions and termed it as '*electromagnetic theory of microstretch elasticity*'. These materials include animal bones and nanomaterials. Books by Eringen and Maugin (1990) and Eringen (1999) on microcontinuum and electrodynamic theories are excellent monographs on this pertinent area of research.

Recently, Khurana and Tomar (2007) have explored the possibility of plane waves propagating in an infinite electro-microelastic solid. They found that there exist five plane waves in an infinite electro-microelastic solid namely (i) an independent longitudinal microrotational wave, (ii) two sets of coupled longitudinal waves, which are influenced by the electric effect, and (iii) two sets of coupled transverse waves. All these waves are dispersive. The appearance of the two sets of coupled longitudinal waves having the influence of electric effect is new, which reduces to the longitudinal displacement wave of micropolar elasticity in the absence of electric and microstretch effects. In the present paper, we have derived the condition on propagation of each plane wave existing in an electro-microelastic solid. Reflection phenomenon of each set of these coupled waves (i.e., the coupled longitudinal waves and the coupled transverse waves) at a stress free flat surface of an electro-microelastic solid half-space is investigated. The amplitude ratios and the energy ratios of various reflected waves are presented and computed numerically for a specific model. We have also compared the square of phase speeds of various waves at different limiting values of frequency. The square of the phase speeds of various existing waves are computed and their variations are depicted graphically against the frequency ratio. The variations of the square of speeds of both sets of coupled longitudinal waves with frequency ratio is shown for three different cases, namely, $\lambda_2^2 >=< \alpha_0(1+\chi^E)$. The variations of modulus of amplitude and energy ratios against the angle of incidence are computed and shown graphically. The behavior of amplitude ratios with the frequency ratio is also depicted graphically. It is found that their is no dissipation of energy at the boundary surface during reflection. The problem of Parfitt and Eringen (1969) has been reduced as a limiting case of the present formulation.

2. Basic equations and constitutive relations

In the absence of body force, body couple and body microstretch force densities, the field equations in a linear isotropic and homogeneous electro-microelastic solid medium when the current vector **J**, volume charge density q_e, magnetic flux vector **B** and thermal effect T are ignored, reduce to (Eringen, 2004)

$$(c_1^2+c_3^2)\nabla\nabla\cdot\mathbf{u}-(c_2^2+c_3^2)\nabla\times\nabla\times\mathbf{u}+c_3^2\nabla\times\mathbf{\Phi}+\bar{\lambda}_0\nabla\psi=\ddot{\mathbf{u}}, \tag{1}$$

$$(c_4^2+c_5^2)\nabla\nabla\cdot\mathbf{\Phi}-c_4^2\nabla\times\nabla\times\mathbf{\Phi}+\omega_0^2\nabla\times\mathbf{u}-2\omega_0^2\mathbf{\Phi}=\ddot{\mathbf{\Phi}}, \tag{2}$$

$$c_6^2\nabla^2\psi-c_7^2\psi-c_8^2\nabla\cdot\mathbf{u}+c_9^2\nabla\cdot\mathbf{E}=\ddot{\psi}, \tag{3}$$

$$(1+\chi^E)\nabla\cdot\mathbf{E}+\lambda_2\nabla^2\psi=0, \tag{4}$$

$$\nabla\times\mathbf{E}=0, \tag{5}$$

where $c_1^2=(\lambda+2\mu)/\rho$, $c_2^2=\mu/\rho$, $c_3^2=K/\rho$, $c_4^2=\gamma/\rho j$, $c_5^2=(\alpha+\beta)/\rho j$, $c_6^2=2\alpha_0/\rho j_0$, $c_7^2=2\lambda_1/3\rho j_0$, $c_8^2=2\lambda_0/3\rho j_0$, $c_9^2=2\lambda_2/\rho j_0$, $\omega_0^2=c_3^2/j$, $\bar{\lambda}_0=\lambda_0/\rho$, λ and μ are Lame's constants; K, α, β and γ are micropolar constants; λ_0, λ_1 and α_0 are microstretch constants; ρ is the density of the medium, j and j_0 are constants, ψ is

the scalar microstretch, **u** and **Φ** are the displacement and microrotation vectors, respectively; **E** is the electric field vector, χ^E is the dielectric susceptibility and the superposed dots on the right hand sides of Eqs. (1)–(3) indicate the double temporal derivative. Note that equation (7.8a) in Eringen (2004) is misprint.

With the above considerations, the force stress tensor t_{kl}, the couple stress tensor m_{kl}, the microstretch couple m_k and the dielectric displacement vector D_k for an electro-microelastic solid medium are given by (Eringen, 2004)

$$t_{kl} = (\lambda_0\psi + \lambda u_{r,r})\delta_{kl} + \mu(u_{k,l} + u_{l,k}) + K(u_{l,k} - e_{klr}\Phi_r), \tag{6}$$

$$m_{kl} = \alpha\Phi_{r,r}\delta_{kl} + \beta\Phi_{k,l} + \gamma\Phi_{l,k} + b_0 e_{lkm}\psi_{,m}, \tag{7}$$

$$m_k = \alpha_0\psi_{,k} + \lambda_2 E_k + b_0 e_{klm}\Phi_{l,m}, \tag{8}$$

$$D_k = (1+\chi^E)E_k + \lambda_2\psi_{,k} + \lambda_3 e_{klm}\Phi_{l,m}, \tag{9}$$

where λ_2 and λ_3 are the coupling constants corresponding to dielectric-microstretch and dielectric-microrotation effects, respectively, b_0 is an elastic moduli corresponding to microstretch and e_{klm} is the permutation symbol.

The following inequalities among the material moduli are the necessary and sufficient conditions for the strain energy density to be non-negative (Eringen, 1999)

$$3\lambda + 2\mu + K \geqslant \frac{3\lambda_0^2}{\lambda_1}, \quad 2\mu + K \geqslant 0, \quad K \geqslant 0, \quad 3\alpha + \beta + \gamma \geqslant 0, \quad \gamma + \beta \geqslant 0, \quad \gamma - \beta \geqslant 0,$$
$$\alpha_0 \geqslant 0, \quad \lambda_1 \geqslant 0, \quad \chi^E \geqslant 0. \tag{10}$$

Introducing the scalar potentials q, ξ and ϵ; the vector potentials **U** and **Π**, as follows

$$\mathbf{u} \equiv \nabla q + \nabla \times \mathbf{U}, \quad \nabla \cdot \mathbf{U} = 0, \tag{11}$$

$$\mathbf{\Phi} \equiv \nabla\xi + \nabla \times \mathbf{\Pi}, \quad \nabla \cdot \mathbf{\Pi} = 0, \tag{12}$$

$$\mathbf{E} \equiv -\nabla\epsilon. \tag{13}$$

Inserting Eq. (13) into Eqs. (4) and (5), we see that Eq. (5) is identically satisfied and Eq. (4) reduces to

$$\nabla^2\epsilon = \frac{\lambda_2}{1+\chi^E}\nabla^2\psi. \tag{14}$$

On substituting Eqs. (11)-(12) into Eqs. (1)–(3) and using (14), we obtain

$$(c_1^2 + c_3^2)\nabla^2 q + \bar{\lambda}_0\psi = \ddot{q}, \tag{15}$$

$$(c_6^2 - c_{10}^2)\nabla^2\psi - c_7^2\psi - c_8^2\nabla^2 q = \ddot{\psi}, \tag{16}$$

$$(c_2^2 + c_3^2)\nabla^2\mathbf{U} + c_3^2\nabla \times \mathbf{\Pi} = \ddot{\mathbf{U}}, \tag{17}$$

$$c_4^2\nabla^2\mathbf{\Pi} - 2\omega_0^2\mathbf{\Pi} + \omega_0^2\nabla \times \mathbf{U} = \ddot{\mathbf{\Pi}}, \tag{18}$$

$$(c_4^2 + c_5^2)\nabla^2\xi - 2\omega_0^2\xi = \ddot{\xi}, \tag{19}$$

where $c_{10}^2 = \frac{2\lambda_2^2}{\rho j_0(1+\chi^E)}$. We note that Eq. (14) is coupled in scalar potentials ϵ and ψ, Eqs. (15) and (16) are coupled in scalar potentials q and ψ, Eqs. (17) and (18) are coupled in vector potentials **U** and **Π** and Eq. (19) is uncoupled in scalar potential ξ.

3. Wave propagation

Keeping the same notations of Khurana and Tomar (2007) of various entities involved here, the phase speeds of two sets of '*coupled longitudinal waves*' each consisting of a '*longitudinal displacement wave*' and a '*longitudinal microstretch wave*' satisfy the equation given by (Khurana and Tomar, 2007)

$$AV^4 - BV^2 + C = 0, \tag{20}$$

where $A = 1 - \frac{\lambda_1\Omega}{3K}\left(\frac{j}{j_0}\right)$, $B = \left(c_1^2 + c_3^2 - \frac{\lambda_0\bar{\lambda}_0}{\lambda_1}\right)A + c_6^2 - c_{10}^2 + \frac{\lambda_0\bar{\lambda}_0}{\lambda_1}$, $C = (c_1^2 + c_3^2)(c_6^2 - c_{10}^2)$ and $\Omega = \frac{2\omega_0^2}{\omega^2}$.

The roots of Eq. (20) are given by

$$V_{1,2}^2 = \frac{1}{2A}(B \pm \sqrt{B^2 - 4AC}), \tag{21}$$

where '+' and '−' signs correspond to V_1^2 and V_2^2, respectively. Since V_1^2 and V_2^2 expressed in Eq. (21) depend upon ω, λ_2 and χ^E, therefore, both the coupled longitudinal waves corresponding to phase speeds V_1 and V_2 are dispersive in nature and are influenced by the electric effect.

Eqs. (17) and (18) represent two sets of '*coupled transverse waves*' propagating with phase speeds V_3 and V_4 and Eq. (19) represents a '*longitudinal microrotational wave*' propagating with phase speed V_5. The expressions of their phase speeds are given by (Parfitt and Eringen, 1969)

$$V_{3,4}^2 = \frac{1}{2(1-\Omega)}\left\{\varepsilon \pm \sqrt{\varepsilon^2 - 4c_4^2(1-\Omega)(c_2^2+c_3^2)}\right\}, \tag{22}$$

$$V_5^2 = (c_4^2 + c_5^2) + \frac{2\omega_0^2}{k^2}, \tag{23}$$

where $\varepsilon = c_4^2 + c_2^2(1-\Omega) + c_3^2(1-\Omega/2)$ and Ω is defined earlier. Each set of '*coupled transverse waves*' refers to two motions, the transverse displacement and the transverse microrotation normal to it and are propagating at the same speed.

Parfitt and Eringen (1969) have shown that the set of coupled transverse waves traveling with speed V_3 and the longitudinal microrotational wave traveling with speed V_5 will propagate only if $\omega > \sqrt{2}\omega_0$, below which they degenerate into distance decaying sinusoidal vibrations. They have also compared the speed of each wave with the phase speeds of other waves existing in the medium at different values of ω. For consistent solution of V_3^2 and V_4^2, the requirement of an additional inequality given by $c_4^2 \geqslant c_2^2 + c_3^2$, i.e.,

$$\frac{\gamma}{j} \geqslant \mu + K, \tag{24}$$

is mentioned, in particular.

The sets of coupled longitudinal waves traveling with speeds $V_{1,2}$ and the sets of coupled transverse waves traveling with speeds $V_{3,4}$, respectively, satisfy the following phonon dispersion relations given by

$$\omega^4 - \left[(c_1^2 + c_3^2 + c_6^2 - c_{10}^2)k^2 + c_7^2\right]\omega^2 + \left[\left(c_1^2 + c_3^2 - \frac{\lambda_0\bar{\lambda}_0}{\lambda_1}\right)c_7^2 + (c_1^2 + c_3^2)(c_6^2 - c_{10}^2)k^2\right]k^2 = 0,$$

$$\omega^4 - \left[2\omega_0^2 + (c_2^2 + c_3^2 + c_4^2)k^2\right]\omega^2 + \left[(2c_2^2 + c_3^2)\omega_0^2 + (c_2^2 + c_3^2)c_4^2k^2\right]k^2 = 0.$$

Now, we shall discuss the behavior of phase speeds V_1 and V_2 at different limiting values of ω and the condition on their existence. If the quantities V_1^2 and V_2^2 are positive, then the corresponding waves will travel with finite speeds in the medium. However, if any one of V_1^2 and V_2^2 or both are negative then the corresponding wave will degenerate into distance decaying sinusoidal vibrations in the medium. It can be seen that the discriminant of Eq. (20), i.e., $B^2 - 4AC$, given by

$$\left[(c_1^2 + c_3^2)\left(1 - \frac{\lambda_1\Omega}{3K}\left(\frac{j}{j_0}\right)\right) - (c_6^2 - c_{10}^2) + \frac{\lambda_0\bar{\lambda}_0\Omega}{3K}\left(\frac{j}{j_0}\right)\right]^2 + \frac{4\lambda_0\bar{\lambda}_0\Omega}{3K}\left(\frac{j}{j_0}\right)(c_6^2 - c_{10}^2)$$

is non-negative for all positive values of ω provided $c_6^2 - c_{10}^2 \geqslant 0$, i.e., $C \geqslant 0$. Therefore, to obtain V_1 and V_2 to be real, we shall choose the values of parameters in such a way that the discriminant $B^2 - 4AC$ is always greater than zero. The subsequent analysis will decide the situations where the corresponding motions are physically acceptable. It can be seen

(i) When $C > 0$, then V_1^2 is positive for $A > 0$, and negative for $A < 0$, while V_2^2 is positive and finite for all non-zero values of A.
(ii) When $C < 0$, then V_1^2 is positive for all non-zero values of A, while V_2^2 is positive for $A < 0$, and negative for $A > 0$.
(iii) When $A = 0$ and $C > 0$, then V_1^2 is infinite and V_2^2 is finite and positive.
(iv) When $A = 0$ and $C < 0$, then V_1^2 is finite and positive provided $c_6^2 - c_{10}^2 + \frac{\lambda_0\bar{\lambda}_0}{\lambda_1} < 0$, and V_2^2 is infinite.

Now we shall discuss the existence of the waves propagating with phase speeds V_1 and V_2 at different limiting values of ω.

Case I: When $c_6^2 - c_{10}^2 \geqslant 0$

(i) If $\Omega \to 0$ then $\omega \to \infty$, Eq. (21) yields

$$V_1^2 = c_1^2 + c_3^2, \quad V_2^2 = c_6^2 - c_{10}^2. \tag{25}$$

Thus for high frequency waves, both V_1^2 and V_2^2 are finite and positive.

(ii) If $\Omega \to \infty$ then $\omega \to 0$, Eq. (21) gives

$$V_1^2 = 0, \quad V_2^2 = c_1^2 + c_3^2 - \frac{\lambda_0\bar{\lambda}_0}{\lambda_1}. \tag{26}$$

Thus for low frequency waves, V_1^2 vanishes whereas V_2^2 is finite. Owing to the first inequality given in (10), it can be seen that V_2^2 is positive.

(iii) If $\Omega \to \frac{3K}{\lambda_1}\left(\frac{j_0}{j}\right)$ then $\omega \to \omega_c\left(=\sqrt{\frac{2\lambda_1}{3K}\left(\frac{j}{j_0}\right)}\omega_0\right)$, Eq. (21) yields $V_1^2 \to \infty$ when $\omega \to \omega_c^+$, $V_1^2 \to -\infty$ when $\omega \to \omega_c^-$ and

$$\lim_{\omega\to\omega_c} V_2^2 = \frac{(c_6^2 - c_{10}^2)(c_1^2 + c_3^2)}{c_6^2 - c_{10}^2 + \frac{\lambda_0\bar{\lambda}_0}{\lambda_1}}. \tag{27}$$

Thus at $\omega = \omega_c$, we see that V_1^2 is infinite and V_2^2 is finite and positive. It can be seen that the quantity $A >=< 0$ accordingly as $\omega >=< \omega_c$. Consequently, the phase speed V_1 is real when $\omega > \omega_c$, infinite when $\omega = \omega_c$, and imaginary when $\omega < \omega_c$. Thus, the frequency ω_c acts as cutoff frequency for the wave propagating with speed V_1.

Case II: When $c_6^2 - c_{10}^2 < 0$

(i) If $\Omega \to 0$ then $\omega \to \infty$, Eq. (21) yields

$$V_1^2 = c_1^2 + c_3^2, \quad V_2^2 = -(c_{10}^2 - c_6^2). \tag{28}$$

Thus, for high frequency waves, V_1^2 is finite and positive, while V_2^2 is negative.

(ii) If $\Omega \to \infty$ then $\omega \to 0$, V_1^2 and V_2^2 given by Eq. (21) will remain same as obtained in **Case (I)** and given in (26).

(iii) If $\Omega \to \frac{3K}{\lambda_1}\left(\frac{j_0}{j}\right)$ then $\omega \to \omega_c\left(=\sqrt{\frac{2\lambda_1}{3K}\left(\frac{j}{j_0}\right)}\omega_0\right)$, Eq. (21) gives $V_2^2 \to \infty$ when $\omega \to \omega_c^-$, $V_2^2 \to -\infty$ when $\omega \to \omega_c^+$ and

$$\lim_{\omega\to\omega_c} V_1^2 = \frac{(c_6^2 - c_{10}^2)(c_1^2 + c_3^2)}{c_6^2 - c_{10}^2 + \frac{\lambda_0\bar{\lambda}_0}{\lambda_1}}. \tag{29}$$

Thus, V_1^2 is positive provided $c_6^2 - c_{10}^2 + \frac{\lambda_0\bar{\lambda}_0}{\lambda_1} < 0$ and V_2^2 is infinite when $\omega \to \omega_c$.

In order to get an idea of the dispersion curves of V_1^2 and V_2^2 with respect to ω, let us look at the possibility of intersection of curves of V_1^2 and V_2^2 at finite and infinite values of ω. Firstly, if they intersect at $\omega \to \infty$, then $V_1^2(\infty) = V_2^2(\infty)$. In this limiting case, the discriminant of Eq. (20) must vanish, that is

$$\lim_{\Omega\to 0}\left[(c_1^2 + c_3^2)\left(1 - \frac{\lambda_1\Omega}{3K}\left(\frac{j}{j_0}\right)\right) - (c_6^2 - c_{10}^2) + \frac{\lambda_0\bar{\lambda}_0\Omega}{3K}\left(\frac{j}{j_0}\right)\right]^2 + \frac{4\lambda_0\bar{\lambda}_0\Omega}{3K}\left(\frac{j}{j_0}\right)(c_6^2 - c_{10}^2) = 0.$$

This yields $c_1^2 + c_3^2 = c_6^2 - c_{10}^2$. This is the condition for consistency of V_1^2 and V_2^2 when $\omega \to \infty$. Secondly, it can be seen that V_1^2 and V_2^2 are not consistent for finite values of ω. Assuming that for some finite value of ω, say $\omega = \omega^*$, we have $V_1^2(\omega^*) = V_2^2(\omega^*)$. This means that the discriminant of Eq. (20) must be equal to zero at $\omega = \omega^*$, but we have already seen that the discriminant is positive and non-zero for all values of $\omega > \omega_c$. Thus, in general, $V_1^2(\omega) > V_2^2(\omega)$ for all positive values of $\omega > \omega_c$. Now, let us compare the magnitudes of V_1^2 and V_2^2

for $\omega > \omega_c$. For $\omega > \omega_c$ (including $\omega \to \infty$), we have $V_1^2 \geqslant V_2^2$. This implies $c_1^2 + c_3^2 \geqslant c_6^2 - c_{10}^2$, which yields the following inequality

$$\frac{2}{j_0}\left(\alpha_0 - \frac{\lambda_2^2}{1+\chi^E}\right) \leqslant \lambda + 2\mu + K \tag{30}$$

Hence, this inequality among the elastic moduli must be satisfied for the consistency of V_1^2 and V_2^2. On comparing the expressions of V_1^2 given in Eqs. (25) and (26), it is easy to see that $V_1^2(0) < V_1^2(\infty)$. Using first inequality of (10), it follows that $V_2^2(0) > V_1^2(0)$ and from inequality (30), we have $V_2^2(\infty) \leqslant V_1^2(\infty)$.

In order to compare the relative magnitudes of V_1^2 with V_3^2 and V_4^2 when $\omega \to 0$, we compare Eq. (26) with equations (48a, b) of Parfitt and Eringen (1969). It is seen that $V_1^2(0) = V_3^2(0)$ and $V_1^2(0) < V_4^2(0)$. Similarly, comparing V_2^2 with V_3^2 and V_4^2 when $\omega \to 0$, it is clear that $V_2^2(0) > V_3^2(0)$ and using the inequality $3\lambda + 2\mu + K \geqslant \frac{3\lambda_0^2}{\lambda_1}$ from (10), we get $V_2^2(0) > V_4^2(0)$.

Next, to compare their relative magnitudes when $\omega \to \infty$, we have from Eq. (25) and equations (47a, b) of Parfitt and Eringen (1969) that $V_1^2 = c_1^2 + c_3^2, V_2^2 = c_6^2 - c_{10}^2, V_3^2 = c_4^2$, and $V_4^2 = c_2^2 + c_3^2$. If $c_4^2 \leqslant c_1^2 + c_3^2$, then $V_4^2(\infty) \leqslant V_3^2(\infty) \leqslant V_1^2(\infty)$. Using inequality (30), it follows that $V_1^2(\infty) \geqslant V_2^2(\infty)$. A similar comparison of V_2^2 can be made with V_3^2 and V_4^2 when $\omega \to \infty$. Using the inequality (24), we obtain $V_2^2(\infty) \geqslant V_3^2(\infty) \geqslant V_4^2(\infty)$, if the inequality $\frac{2}{j_0}\left(\alpha_0 - \frac{2\lambda_2^2}{1+\chi^E}\right) \geqslant \frac{\gamma}{j}$ holds.

4. Reflection coefficients

Here, we shall discuss the problem of reflection of plane waves when a set of these coupled waves is made incident obliquely at the free plane boundary of an electro-microelastic solid half-space. Let $\Re = \{(x_1, x_3) : -\infty < x_1 < \infty, 0 \leqslant x_3 < \infty\}$ be the region occupied by an electro-microelastic solid half-space with the elastic constants λ, μ, K, γ, α_0, λ_0, b_0, λ_2, χ^E and the density ρ. Let the plane boundary surface of $\Re$ given by $x_3 = 0$ be free from mechanical stresses. The problem is two dimensional in x_1x_3-plane so we can take

$$\mathbf{u} = (u_1, 0, u_3), \quad \mathbf{\Phi} = (0, \phi_2, 0), \quad \frac{\partial}{\partial x_2} \equiv 0, \tag{31}$$

where $\phi_2 = (-\nabla \times \mathbf{\Pi})_{x_2}$. From relation (11), we obtain

$$u_1 = \frac{\partial q}{\partial x_1} - \frac{\partial U_2}{\partial x_3}, \quad u_3 = \frac{\partial q}{\partial x_3} + \frac{\partial U_2}{\partial x_1},$$

where $U_2 = (\mathbf{U})_{x_2}$.

4.1. When a set of coupled longitudinal waves with phase speed V_1 is incident

Consider a set of coupled longitudinal waves of amplitude A_0 propagating with speed V_1 through the medium $\Re$ is made incident at the free plane surface, making an angle θ_0 with the x_3-axis. We take the following reflected waves into consideration to satisfy the boundary conditions at the free plane surface:

(i) Two sets of coupled longitudinal waves of amplitudes $A_{1,2}$ propagating with speeds $V_{1,2}$ and making angles $\theta_{1,2}$ respectively, with the normal.
(ii) Two sets of coupled transverse waves of amplitudes $A_{3,4}$ propagating with speeds $V_{3,4}$ and making angles $\theta_{3,4}$ respectively, with the normal.The relevant potentials in the half-space $\Re$ are given by:

$$\{q, \psi\} = \{1, \zeta_1\}A_0P_0^- + \sum_{p=1,2}\{1, \zeta_p\}A_pP_p^+, \tag{32}$$

$$\{U_2, \phi_2\} = \sum_{p=3,4}\{1, \eta_p\}A_pP_p^+, \tag{33}$$

where $P_0^- = \exp\{\iota k_1(\sin\theta_0 x_1 - \cos\theta_0 x_3) - \iota\omega_1 t\}, P_p^+ = \exp\{\iota k_p(\sin\theta_p x_1 + \cos\theta_p x_3) - \iota\omega_p t\}$, k_p is the wavenumber and $\omega_p(=k_p\ V_p)$ is the circular frequency of the wave propagating with phase speed V_p. The ζ_i's $(i = 1, 2)$ are coupling parameters between q and ψ, and the η_i's $(i = 3, 4)$ are coupling parameters between U_2 and ϕ_2. The expressions of ζ_i's and η_i's are given by (Khurana and Tomar, 2007)

$$\zeta_{1,2} = \frac{\omega^2}{\lambda_0}\left[\frac{c_1^2 + c_3^2}{V_{1,2}^2} - 1\right] \quad \text{and} \quad \eta_{3,4} = \omega_0^2\left[V_{3,4}^2 - \frac{2\omega_0^2}{k_{3,4}^2} - c_4^2\right]^{-1}.$$

Using Eqs. (11)–(13) into Eqs. (6)–(8), the requisite components of stresses in the medium $\Re$ are given by

$$\begin{aligned} t_{33} &= (\lambda + 2\mu + K)q_{,33} + (2\mu + K)U_{2,13} + \lambda q_{,11} + \lambda_0\psi, \\ t_{31} &= (2\mu + K)q_{,13} - (\mu + K)U_{2,33} + \mu U_{2,11} - K\phi_2, \\ m_{32} &= \gamma\phi_{2,3} + b_0\psi_{,1}, \quad m_3 = \left(\alpha_0 - \frac{\lambda_2^2}{1 + \chi^E}\right)\psi_{,3} - b_0\phi_{2,1}. \end{aligned} \tag{34}$$

Since the boundary of the half-space $\Re$ is mechanically stress free, therefore, the appropriate boundary conditions at the boundary surface are the vanishing of force stress, couple stress and microstretch couple. Mathematically, these boundary conditions can be written as:

$$t_{33} = t_{31} = m_{32} = m_3 = 0, \quad \text{at } x_3 = 0. \tag{35}$$

These potentials given in Eqs. (32)-(33) will satisfy the above boundary conditions at $x_3 = 0$ if $\omega = \omega_1 = \omega_2 = \omega_3 = \omega_4$, $k_1\sin\ \theta_0 = k_1\sin\theta_1 = k_2\sin\theta_2 = k_3\sin\theta_3 = k_4\sin\theta_4$ and

$$\begin{aligned} &\left[\lambda + (2\mu + K)\cos^2\theta_0 - \frac{\lambda_0\zeta_1}{k_1^2}\right]k_1^2 A_0 + \sum_{p=1,2}\left[\lambda + (2\mu + K)\cos^2\theta_p - \frac{\lambda_0\zeta_p}{k_p^2}\right]k_p^2 A_p \\ &\quad + (2\mu + K)\sum_{p=3,4}\sin\theta_p\cos\theta_p k_p^2 A_p = 0, \end{aligned} \tag{36}$$

$$(2\mu + K)\sin\theta_0\cos\theta_0 k_1^2 A_0 - (2\mu + K)\sum_{p=1,2}\sin\theta_p\cos\theta_p k_p^2 A_p + \sum_{p=3,4}\left[\mu\cos 2\theta_p + K\cos^2\theta_p - \frac{K\eta_p}{k_p^2}\right]k_p^2 A_p = 0, \tag{37}$$

$$b_0\zeta_1\sin\theta_0 k_1 A_0 + b_0\sum_{p=1,2}\zeta_p\sin\theta_p k_p A_p + \gamma\sum_{p=3,4}\eta_p\cos\theta_p k_p A_p = 0, \tag{38}$$

$$\left(\alpha_0 - \frac{\lambda_2^2}{1 + \chi^E}\right)\left(\zeta_1\cos\theta_0 k_1 A_0 - \sum_{p=1,2}\zeta_p\cos\theta_p k_p A_p\right) + b_0\sum_{p=3,4}\eta_p\sin\theta_p k_p A_p = 0. \tag{39}$$

Eqs. (36)–(39) enable us to provide the amplitude ratios of various reflected waves. These equations can be written in matrix form as

$$[a_{ij}][Z] = [M], \tag{40}$$

where $[a_{ij}]$ is a 4×4 matrix, [Z] and [M] are column matrices. The elements of coefficient matrix $[a_{ij}]$ can be written in non-dimensional form as

$$a_{11}=1,\quad a_{12}=\left[\lambda+\Delta_2(1-v_{21}^2\sin^2\theta_0)-\frac{\lambda_0\zeta_2}{k_2^2}\right]/\Delta_1 v_{21}^2,$$

$$a_{1p}=\Delta_2\sin\theta_0\sqrt{1-v_{p1}^2\sin^2\theta_0}/\Delta_1 v_{p1},$$

$$a_{21}=\sin\theta_0\cos\theta_0,\quad a_{22}=\sin\theta_0\sqrt{1-v_{21}^2\sin^2\theta_0}/v_{21},$$

$$a_{2p}=-\left[\mu(1-2v_{p1}^2\sin^2\theta_0)+K(1-v_{p1}^2\sin^2\theta_0)-\frac{K\eta_p}{k_p^2}\right]/\Delta_2 v_{p1}^2,$$

$$a_{31}=\sin\theta_0,\quad a_{32}=\zeta_2\sin\theta_0/\zeta_1,\quad a_{3p}=\gamma\eta_p\sqrt{1-v_{p1}^2\sin^2\theta_0}/b_0\zeta_1 v_{p1},$$

$$a_{41}=\cos\theta_0,\quad a_{42}=\zeta_2\sqrt{1-v_{21}^2\sin^2\theta_0}/\zeta_1 v_{21},$$

$$a_{4p}=-b_0\eta_p\sin\theta_0/(\alpha_0-\frac{\lambda_2^2}{1+\chi^E})\zeta_1,\quad p=3,4,$$

where $\Delta_1=\left[\lambda+\Delta_2\cos^2\theta_0-\frac{\lambda_0\zeta_1}{k_1^2}\right]$, $\Delta_2=2\mu+K$, $v_{m1}=\frac{V_m}{V_1}(m=2,3,4)$, $[M]=[-1,\ \sin\theta_0\cos\theta_0,\ -\sin\theta_0,\ \cos\theta_0]^{\mathrm{t}}$, $[Z]=[Z_1,\ Z_2,\ Z_3,\ Z_4]^{\mathrm{t}}$ and 't' in the superscript represents the transpose of the matrix. $Z_r=\frac{A_r}{A_0}(r=1,2,3,4)$ are the reflection coefficients for an incident set of coupled longitudinal waves traveling with speed V_1.

Now, we shall discuss the partitioning of incident energy between various reflected waves at the free plane surface ($x_3=0$). The rate of energy transmission per unit area denoted by P^* is given by (Achenbach, 1973)

$$P^*=t_{33}\dot{u}_3+t_{31}\dot{u}_1+m_{32}\dot{\phi}_2+m_3\dot{\psi}. \tag{41}$$

The expressions of energy ratios $E_i^r(i=1,2,3,4)$ are

$$E_1^r=Z_1^2,\quad E_2^r=Z_2^2P_1\left[\lambda+2\mu+K-\frac{\lambda_0\zeta_2}{k_2^2}-\frac{\alpha_0\zeta_2^2}{k_2^2}+\frac{\lambda_2^2\zeta_2^2}{(1+\chi^E)k_2^2}\right]k_2^3\cos\theta_2,$$

$$E_{3,4}^r=Z_{3,4}^2P_1\left[\mu+K-\frac{\eta_{3,4}}{k_{3,4}^2}(\gamma\eta_{3,4}+K)\right]k_{3,4}^3\cos\theta_{3,4},$$

where $P_1=\left[\left(\lambda+2\mu+K-\frac{\lambda_0\zeta_1}{k_1^2}-\frac{\alpha_0\zeta_1^2}{k_1^2}+\frac{\lambda_2^2\zeta_1^2}{(1+\chi^E)k_1^2}\right)k_1^3\cos\theta_0\right]^{-1}$. Each energy ratio $E_i^r(i=1,2,3,4)$ gives the rate of energy transmission at the free plane surface for the respective reflected wave to the rate of energy transmission for an incident set of coupled longitudinal waves propagating with speed V_1.

4.2. When a set of coupled longitudinal waves with phase speed V_2 is incident

Let a set of coupled longitudinal waves of amplitude A_0 propagating with speed V_2 be incident at the free plane surface $x_3=0$. In this case, we shall consider the same set of reflected waves as considered in the previous case. Following the same procedure as above, we obtain a matrix equation similar to (40) with the following modified values

$$a_{11}=\left[\lambda+\Delta_2(1-v_{12}^2\sin^2\theta_0)-\frac{\lambda_0\zeta_1}{k_1^2}\right]/\Delta_3 v_{12}^2,\quad a_{12}=1,$$

$$a_{1p}=\Delta_2\sin\theta_0\sqrt{1-v_{p2}^2\sin^2\theta_0}/\Delta_3 v_{p2},$$

$$a_{21} = \sin\theta_0\sqrt{1 - v_{12}^2\sin^2\theta_0}/v_{12}, a_{22} = \sin\theta_0\cos\theta_0,$$
$$a_{2p} = -\left[\mu(1 - 2v_{p2}^2\sin^2\theta_0) + K(1 - v_{p2}^2\sin^2\theta_0) - \frac{K\eta_p}{k_p^2}\right]/\Delta_2 v_{p2}^2,$$
$$a_{31} = \zeta_1\sin\theta_0/\zeta_2, \quad a_{32} = \sin\theta_0, \quad a_{3p} = \gamma\eta_p\sqrt{1 - v_{p2}^2\sin^2\theta_0}/b_0\zeta_2 v_{p2},$$
$$a_{41} = \zeta_1\sqrt{1 - v_{12}^2\sin^2\theta_0}/\zeta_2 v_{12}, \quad a_{42} = \cos\theta_0,$$
$$a_{4p} = -b_0\eta_p\sin\theta_0/\left(\alpha_0 - \frac{\lambda_2^2}{1+\chi^E}\right)\zeta_2, \quad p = 3,4,$$

where $\Delta_3 = \left[\lambda + \Delta_2\cos^2\theta_0 - \frac{\lambda_0\zeta_2}{k_2^2}\right]$, $v_{m2} = \frac{V_m}{V_2}(m = 1,3,4)$ and Δ_2 is defined earlier. The matrices $[Z]$ and $[M]$ would remain unaltered and $Z_r = \frac{A_r}{A_0}(r = 1,2,3,4)$ will now denote the reflection coefficients for an incident set of coupled longitudinal waves propagating with speed V_2. In this case, the expressions for energy ratios of various reflected waves are given as

$$E_1^r = Z_1^2 P_2\left[\lambda + 2\mu + K - \frac{\lambda_0\zeta_1}{k_1^2} - \frac{\alpha_0\zeta_1^2}{k_1^2} + \frac{\lambda_2^2\zeta_1^2}{(1+\chi^E)k_1^2}\right]k_1^3\cos\theta_1,$$
$$E_2^r = Z_2^2, \quad E_{3,4}^r = Z_{3,4}^2 P_2\left[\mu + K - \frac{\eta_{3,4}}{k_{3,4}^2}(\gamma\eta_{3,4} + K)\right]k_{3,4}^3\cos\theta_{3,4},$$

where $P_2 = \left[\left(\lambda + 2\mu + K - \frac{\lambda_0\zeta_2}{k_2^2} - \frac{\alpha_0\zeta_2^2}{k_2^2} + \frac{\lambda_2^2\zeta_2^2}{(1+\chi^E)k_2^2}\right)k_2^3\cos\theta_0\right]^{-1}$. Each energy ratio $E_i^r(1,2,3,4)$ will now represents the rate of energy transmission at the free plane boundary surface for respective reflected wave to the energy transmission for an incident set of coupled longitudinal waves with speed V_2.

4.3. When a set of coupled transverse waves with phase speed V_3 is incident

We shall now study the reflection at a free plane surface of $\Re$ when a set of coupled transverse waves propagating with phase speed V_3 and having amplitude A_0 is incident at an angle θ_0 with the normal. The geometry of the problem and the set of reflected waves will remain same as considered in the previous cases of incident sets of coupled longitudinal waves. Also, the boundary conditions will be the same as given in Eq. (35). In the present formulation, the relevant potentials in medium $\Re$ are given by:

$$\{U_2, \phi_2\} = \{1, \eta_3\}A_0 Q_0^- + \sum_{p=3,4}\{1, \eta_p\}A_p P_p^+, \tag{42}$$
$$\{q, \psi\} = \sum_{p=1,2}\{1, \zeta_p\}A_p P_p^+, \tag{43}$$

where $Q_0^- = \exp\{\iota k_3(\sin\theta_0 x_1 - \cos\theta_0 x_3) - \iota\omega_3 t\}$ and P_p^+ is defined earlier.

Using the above potentials into the boundary conditions given in Eq. (35), we obtain the following system of equations:

$$(2\mu + K)\sin\theta_0\cos\theta_0 k_3^2 A_0 - \sum_{p=1,2}\left[\lambda + (2\mu + K)\cos^2\theta_p - \frac{\lambda_0\zeta_p}{k_p^2}\right]k_p^2 A_p$$
$$- (2\mu + K)\sum_{p=3,4}\sin\theta_p\cos\theta_p k_p^2 A_p = 0, \tag{44}$$

$$\left[\mu\cos 2\theta_0 + K\cos^2\theta_0 - \frac{K\eta_3}{k_3^2}\right]k_3^2A_0 - (2\mu+K)\sum_{p=1,2}\sin\theta_p\cos\theta_p k_p^2A_p + \sum_{p=3,4}\left[\mu\cos 2\theta_p + K\cos^2\theta_p - \frac{K\eta_p}{k_p^2}\right]k_p^2A_p = 0, \tag{45}$$

$$\gamma\eta_3\cos\theta_0 k_3A_0 - b_0\sum_{p=1,2}\zeta_p\sin\theta_p k_pA_p - \gamma\sum_{p=3,4}\eta_p\cos\theta_p k_pA_p = 0, \tag{46}$$

$$b_0\eta_3\sin\theta_0 k_3A_0 - \left(\alpha_0 - \frac{\lambda_2^2}{1+\chi^E}\right)\sum_{p=1,2}\zeta_p\cos\theta_p k_pA_p + b_0\sum_{p=3,4}\eta_p\sin\theta_p k_pA_p = 0, \tag{47}$$

The system of Eqs. (44)–(47) can be written in matrix form as

$$[b_{ij}][Z] = [X], \tag{48}$$

where $[b_{ij}]$ is a 4×4 matrix, [Z] and [X] are column matrices. Using the modified Snell's law for this case, the elements of coefficient matrix $[b_{ij}]$ can be written as

$$b_{1s} = \left[\lambda + \Delta_2(1 - v_{s3}^2\sin^2\theta_0) - \frac{\lambda_0\zeta_s}{k_s^2}\right]/\Delta_2 v_{s3}^2,$$

$$b_{13} = \sin\theta_0\cos\theta_0, b_{14} = \sin\theta_0\sqrt{1 - v_{43}^2\sin^2\theta_0}/v_{43},$$

$$b_{2s} = \Delta_2\sin\theta_0\sqrt{1 - v_{s3}^2\sin^2\theta_0}/\Delta_4 v_{s3}, b_{23} = -1,$$

$$b_{24} = -\left[\mu(1 - 2v_{43}^2\sin^2\theta_0) + K(1 - v_{43}^2\sin^2\theta_0) - \frac{K\eta_4}{k_4^2}\right]/\Delta_4 v_{43}^2,$$

$$b_{3s} = b_0\zeta_s\sin\theta_0/\gamma\eta_3, \quad b_{33} = \cos\theta_0, \quad b_{34} = \eta_4\sqrt{1 - v_{43}^2\sin^2\theta_0}/\eta_3 v_{43},$$

$$b_{4s} = \zeta_s\left(\alpha_0 - \frac{\lambda_2^2}{1+\chi^E}\right)\sqrt{1 - v_{s3}^2\sin^2\theta_0}/b_0\eta_3 v_{s3},$$

$$b_{43} = -\sin\theta_0, \quad b_{44} = -\eta_4\sin\theta_0/\eta_3, \quad s = 1, 2,$$

where $\Delta_4 = \left[\mu\cos 2\theta_0 + K\cos^2\theta_0 - \frac{K\eta_3}{k_3^2}\right]$, $v_{m3} = \frac{V_m}{V_3}(m = 1, 2, 4)$, $[X] = [\sin\theta_0\cos\theta_0, 1, \cos\theta_0, \sin\theta_0]^t$, $[Z] = [Z_1, Z_2, Z_3, Z_4]^t$ and $Z_r(r = 1, 2, 3, 4)$ defined earlier are now the reflection coefficients for an incident set of coupled transverse waves traveling with speed V_3. Thus, Eq. (48) will enable us to provide the expressions of reflection coefficients in the present case. The expressions for energy ratios $E_i^r(i = 1, 2, 3, 4)$ of various reflected waves in this case are given by

$$E_{1,2}^r = Z_{1,2}^2P_3\left[\lambda + 2\mu + K - \frac{\lambda_0\zeta_{1,2}}{k_{1,2}^2} - \frac{\alpha_0\zeta_{1,2}^2}{k_{1,2}^2} + \frac{\lambda_2^2\zeta_{1,2}^2}{(1+\chi^E)k_{1,2}^2}\right]k_{1,2}^3\cos\theta_{1,2},$$

$$E_3^r = Z_3^2, \quad E_4^r = Z_4^2P_3\left[\mu + K - \frac{\eta_4}{k_4^2}(\gamma\eta_4 + K)\right]k_4^3\cos\theta_4,$$

where $P_3 = \left[\left(\mu + K - \frac{\eta_3}{k_3^2}(\gamma\eta_3 + K)\right)k_3^3\cos\theta_0\right]^{-1}$. Here, each energy ratio E_i^r will give the rate of energy transmitted at the free plane surface for the respective reflected wave to the rate of energy transmitted for an incident coupled transverse waves with speed V_3.

4.4. When a set of coupled transverse waves with phase speed V_4 is incident

Following the same procedure as above, we obtain a matrix equation similar to Eq. (48) with the following values

$$b_{1s} = \left[\lambda + \Delta_2(1 - v_{s4}^2 \sin^2\theta_0) - \frac{\lambda_0\zeta_s}{k_s^2}\right]/\Delta_2 v_{s4}^2,$$

$$b_{13} = \sin\theta_0\sqrt{1 - v_{34}^2\sin^2\theta_0}/v_{34}, \quad b_{14} = \sin\theta_0\cos\theta_0,$$

$$b_{2s} = \Delta_2\sin\theta_0\sqrt{1 - v_{s4}^2\sin^2\theta_0}/\Delta_5 v_{s4},$$

$$b_{23} = -\left[\mu(1 - 2v_{34}^2\sin^2\theta_0) + K(1 - v_{34}^2\sin^2\theta_0) - \frac{K\eta_3}{k_3^2}\right]/\Delta_5 v_{34}^2,$$

$$b_{24} = -1, \quad b_{3s} = b_0\zeta_s\sin\theta_0/\gamma\eta_4, \quad b_{33} = \eta_3\sqrt{1 - v_{34}^2\sin^2\theta_0}/\eta_4 v_{34},$$

$$b_{34} = \cos\theta_0, \quad b_{4s} = \zeta_s(\alpha_0 - \frac{\lambda_2^2}{1+\chi^E})\sqrt{1 - v_{s4}^2\sin^2\theta_0}/b_0\eta_4 v_{s4},$$

$$b_{43} = -\eta_3\sin\theta_0/\eta_4, \quad b_{44} = -\sin\theta_0, s = 1, 2,$$

where $\Delta_5 = \left[\mu\cos 2\theta_0 + K\cos^2\theta_0 - \frac{K\eta_4}{k_4^2}\right]$, $v_{m4} = \frac{V_m}{V_4}(m = 1, 2, 3)$, and the matrices $[Z]$ and $[X]$ have same values as in the matrix Eq. (48). $Z_r(r = 1, 2, 3, 4)$ defined earlier are now the reflection coefficients for an incident set of coupled transverse waves traveling with phase speed V_4. The expressions for energy ratios $E_i^r(i = 1, 2, 3, 4)$ of various reflected waves in this case, are given by

$$E_{1,2}^r = Z_{1,2}^2 P_4\left[\lambda + 2\mu + K - \frac{\lambda_0\zeta_{1,2}}{k_{1,2}^2} - \frac{\alpha_0\zeta_{1,2}^2}{k_{1,2}^2} + \frac{\lambda_2^2\zeta_{1,2}^2}{(1+\chi^E)k_{1,2}^2}\right]k_{1,2}^3\cos\theta_{1,2},$$

$$E_3^r = Z_3^2 P_4\left[\mu + K - \frac{\eta_3}{k_3^2}(\gamma\eta_3 + K)\right]k_3^3\cos\theta_3, \quad E_4^r = Z_4^2,$$

where $P_4 = \left[(\mu + K - \frac{\eta_4}{k_4^2}(\gamma\eta_4 + K))k_4^3\cos\theta_0\right]^{-1}$ and each $E_i^r(i = 1, 2, 3, 4)$ will now give the rate of energy transmission of the respective reflected wave to the rate of energy transmission of an incident set of coupled transverse waves propagating with speed V_4.

5. Limiting cases

(i) If we assume that the half-space $\Re$ is free from microstretch and electric effects, then we shall be left with the relevant problem in micropolar elastic solid half-space. In this limiting case, it can be seen that $V_2 = 0$, i.e., the wave propagating with speed V_2 will not appear in the medium. Thus, we obtain $A_2 = 0$ and we note that Eq. (39) is identically satisfied. By making the appropriate changes in the Eqs. (36)–(38), due to consideration of $U_2 = (-\mathbf{U})_{x_2}$ in Parfitt and Eringen (1969), the resulting equations reduce to the equations (75)–(77) of Parfitt and Eringen (1969) for the case of an incident set of coupled longitudinal waves traveling with speed V_1.

Similarly, when a set of coupled transverse waves propagating through the medium with phase speed V_3 becomes incident at the stress free plane boundary surface, then in this limiting case, we see that the Eq. (47) is satisfied identically and Eqs. (44)–(46) reduce to the following equations

$$(2\mu + K)\sin\theta_0\cos\theta_0 k_3^2 A_0 - \left[\lambda + (2\mu + K)\cos^2\theta_1\right]k_1^2 A_1 - (2\mu + K)\sum_{p=3,4}\sin\theta_p\cos\theta_p k_p^2 A_p = 0, \tag{49}$$

$$\left[\mu\cos 2\theta_0 + K\cos^2\theta_0 - \frac{K\eta_3}{k_3^2}\right]k_3^2 A_0 - (2\mu + K)\sin\theta_1\cos\theta_1 k_1^2 A_1 + \sum_{p=3,4}\left[\mu\cos 2\theta_p + K\cos^2\theta_p - \frac{K\eta_p}{k_p^2}\right]k_p^2 A_p = 0, \tag{50}$$

$$\gamma\eta_3 \cos\theta_0 k_3 A_0 - \gamma \sum_{p=3,4} \eta_p \cos\theta_p k_p A_p = 0. \tag{51}$$

(ii) If we assume that the half-space $\Re$ is free from electric effect, then we will be left with the relevant problem in linear homogeneous microstretch elastic solid half-space. In this limiting case, the Eqs. (36)–(39) reduce to

$$\left[\lambda + (2\mu+K)\cos^2\theta_0 - \frac{\lambda_0\zeta_1}{k_1^2}\right]k_1^2 A_0 + \sum_{p=1,2}\left[\lambda + (2\mu+K)\cos^2\theta_p - \frac{\lambda_0\zeta_p}{k_p^2}\right]k_p^2 A_p + (2\mu+K)\sum_{p=3,4}\sin\theta_p\cos\theta_p k_p^2 A_p = 0, \tag{52}$$

$$(2\mu+K)\sin\theta_0\cos\theta_0 k_1^2 A_0 - (2\mu+K)\sum_{p=1,2}\sin\theta_p\cos\theta_p k_p^2 A_p + \sum_{p=3,4}\left[\mu\cos 2\theta_p + K\cos^2\theta_p - \frac{K\eta_p}{k_p^2}\right]k_p^2 A_p = 0, \tag{53}$$

$$b_0\zeta_1 \sin\theta_0 k_1 A_0 + b_0\sum_{p=1,2}\zeta_p \sin\theta_p k_p A_p + \gamma\sum_{p=3,4}\eta_p\cos\theta_p k_p A_p = 0, \tag{54}$$

$$\alpha_0\zeta_1\cos\theta_0 k_1 A_0 - \alpha_0\sum_{p=1,2}\zeta_p\cos\theta_p k_p A_p + b_0\sum_{p=3,4}\eta_p\sin\theta_p k_p A_p = 0. \tag{55}$$

These equations will provide us the reflection coefficients when a set of coupled longitudinal waves propagating with speed V_1 is made incident at the stress free plane surface of microstretch elastic solid half-space.

Similarly, when a set of coupled transverse waves propagating through the medium with speed V_3 is incident at the free surface $x_3 = 0$, then we see that in this limiting case, Eqs. (44)–(47) reduce to

$$(2\mu+K)\sin\theta_0\cos\theta_0 k_3^2 A_0 - \sum_{p=1,2}\left[\lambda + (2\mu+K)\cos^2\theta_p - \frac{\lambda_0\zeta_p}{k_p^2}\right]k_p^2 A_p - (2\mu+K)\sum_{p=3,4}\sin\theta_p\cos\theta_p k_p^2 A_p = 0, \tag{56}$$

$$\left[\mu\cos 2\theta_0 + K\cos^2\theta_0 - \frac{K\eta_3}{k_3^2}\right]k_3^2 A_0 - (2\mu+K)\sum_{p=1,2}\sin\theta_p\cos\theta_p k_p^2 A_p + \sum_{p=3,4}\left[\mu\cos 2\theta_p + K\cos^2\theta_p - \frac{K\eta_p}{k_p^2}\right]k_p^2 A_p = 0, \tag{57}$$

$$\gamma\eta_3\cos\theta_0 k_3 A_0 - b_0\sum_{p=1,2}\zeta_p\sin\theta_p k_p A_p - \gamma\sum_{p=3,4}\eta_p\cos\theta_p k_p A_p = 0, \tag{58}$$

$$b_0\eta_3\sin\theta_0 k_3 A_0 - \alpha_0\sum_{p=1,2}\zeta_p\cos\theta_p k_p A_p + b_0\sum_{p=3,4}\eta_p\sin\theta_p k_p A_p = 0. \tag{59}$$

These equations will provide us the reflection coefficients for the case of an incident set of coupled transverse waves propagating with speed V_3.

6. Numerical results and discussions

In order to examine this study in greater detail, we have computed the square of phase speeds of existing coupled waves, amplitude ratios and energy ratios of various reflected waves, for a particular model. For this purpose, we have taken the following values of relevant parameters:

$\lambda = 7.85\times10^{11}$ dyne/cm^2, $\mu = 6.46\times10^{11}$ dyne/cm^2, $K = 0.0125\times10^{11}$ dyne/cm^2,

$\alpha_0 = 0.085 \times 10^{11}$ dyne, $\lambda_0 = 0.038 \times 10^{11}$ dyne/cm^2, $\lambda_1 = 0.030 \times 10^{11}$ dyne/cm^2, $\lambda_2^2 = 0.3364 \times 10^{11}$ dyne, $j = j_0 = 0.0212$ cm^2, $\rho = 1.9$ gm/cm^3, $\gamma = 0.365 \times 10^{11}$ dyne, $b_0 = 0.096 \times 10^{11}$ dyne, $\chi^E = 318.0$ and $\omega/\omega_0 = 10$ wherever not mentioned.

First, we have computed the square of phase speeds $V_i^2 (i = 1, 2, 3, 4)$ of the existing waves given by Eqs. (21) and (22) at different values of ω/ω_0 ranging from 0.1 to 5.0. They are computed separately for two distinct values of $R(=\gamma/\mu j)$ and are depicted through Figs. 1–4.

Fig. 1 depicts the variation of V_1^2 with the frequency ratio ω/ω_0, at $R = 2.67$ and 5.04. It is found that at both the values of R, V_1^2 is zero initially, it becomes more and more negative with increase in ω/ω_0 until it tends to $-\infty$ as $\omega/\omega_0 \to 1.26$ from left. At $\omega/\omega_0 = 1.26$, there is a sudden jump in the curve and the value of V_1^2 tends to $+\infty$ as $\omega/\omega_0 \to 1.26$ from right. For $\omega/\omega_0 > 1.26$, the value of V_1^2 is positive and decreases gradually to

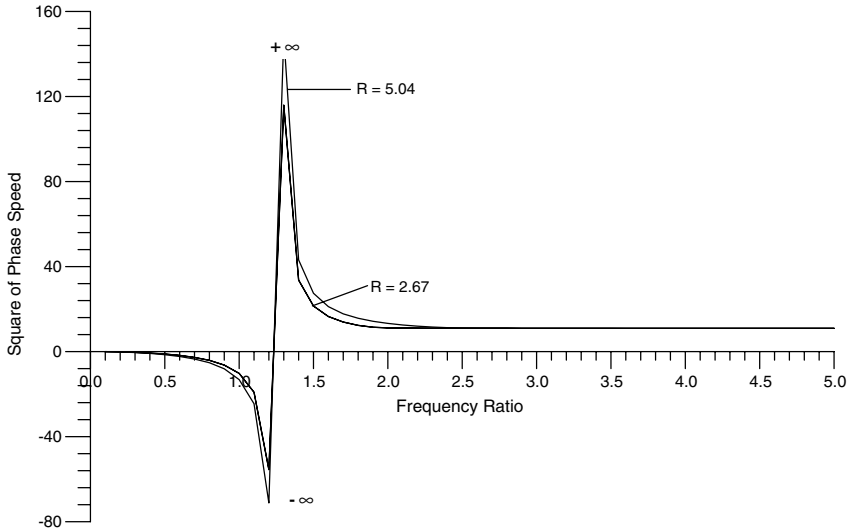

Fig. 1. Variation of V_1^2 with frequency ratio ω/ω_0 $\left(R = \frac{\gamma}{\mu j}\right)$.

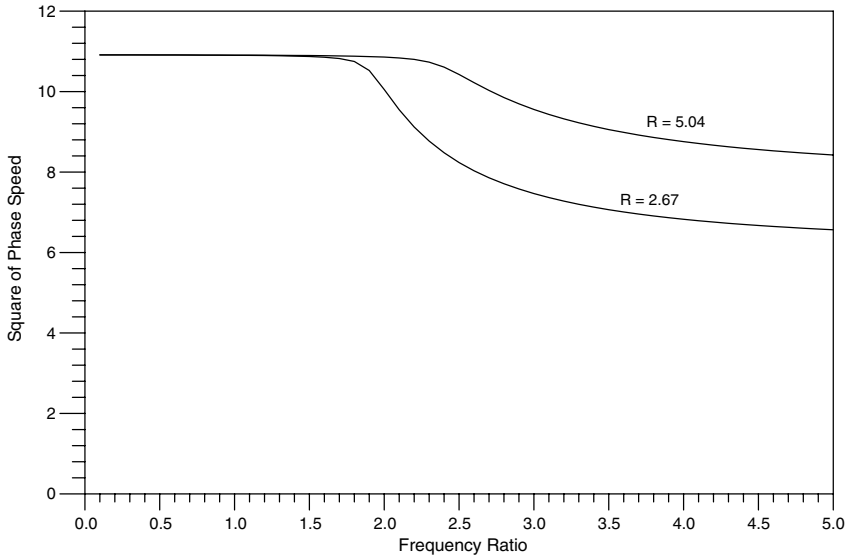

Fig. 2. Variation of V_2^2 with frequency ratio ω/ω_0 $\left(R = \frac{\gamma}{\mu j}\right)$.

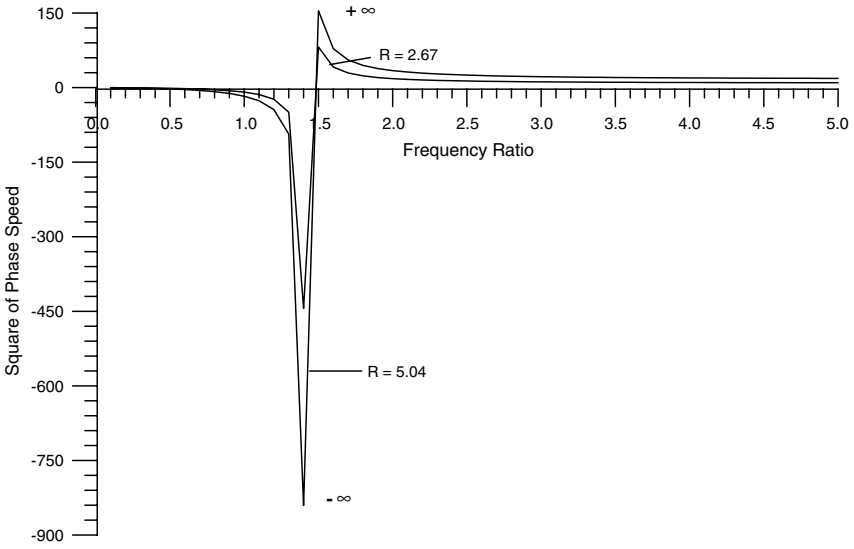

Fig. 3. Variation of V_3^2 with frequency ratio ω/ω_0 $\left(R = \frac{\gamma}{\mu j}\right)$.

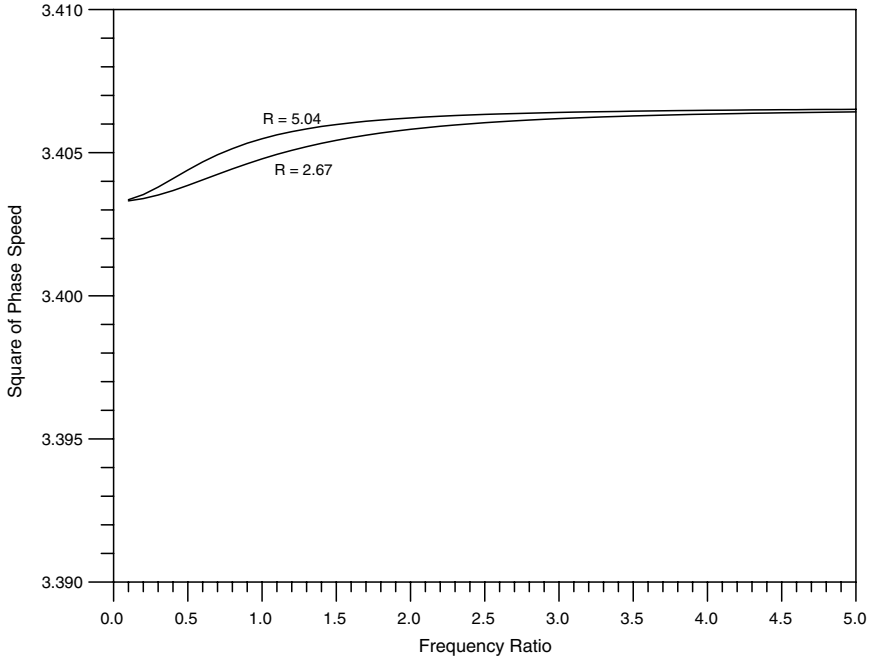

Fig. 4. Variation of V_4^2 with frequency ratio ω/ω_0 $\left(R = \frac{\gamma}{\mu j}\right)$.

some positive and finite value as ω/ω_0 takes larger and larger value. Thus, there is a cutoff frequency for V_1 near the value $\omega = 1.26 \times \omega_0$. This value is same as one can obtain from the formula $\omega = \omega_c = \sqrt{\frac{2\lambda_1}{3K}\left(\frac{j}{J_0}\right)}\omega_0$ derived earlier on substituting the values of respective material constants.

Fig. 2 depicts the variation of V_2^2 with the frequency ratio ω/ω_0 at two different values of R mentioned above. It is found that at both these values of R, V_2^2 is positive and remains almost constant in the range $0 < \omega/\omega_0 \leqslant 1.20$, thereafter, its value decreases with increasing values of frequency ratio.

In Fig. 3, we have plotted V_3^2 against the frequency ratio ω/ω_0 at two different mentioned values of R. It can be noticed from this figure that at these values of R, the behavior of V_3^2 is similar to that of V_1^2 with ω/ω_0.

The value of V_3^2 is negative in the range $0 < \omega/\omega_0 < 1.414$ and is positive in the range $\omega/\omega_0 > 1.414$. Thus, $\omega/\omega_0 = 1.414$ acts as a cutoff frequency for the phase speed V_3, which is the same value as one can obtain from the formula $\omega = \omega_c = \sqrt{2}\omega_0$. In Fig. 4, we have shown the variation of V_4^2 versus the frequency ratio ω/ω_0 at $R = 2.67$ and 5.04. It is found that V_4^2 is positive and its value increases with increase of frequency ratio.

Thus, we conclude that when $c_6^2 - c_{10}^2 > 0$, the waves with phase speeds V_2 and V_4 exist for all positive values of frequency, while there exist a cutoff frequency for the waves propagating with phase speeds V_1 and V_3, below which they degenerate into distance decaying sinusoidal vibrations. However, the value of cutoff frequency for the wave propagating with speed V_1 is different from the value of cutoff frequency for the wave propagating with speed V_3.

In Figs. 5–7, we have compared the dispersion curves of V_1^2 and V_2^2 when $c_6^2 - c_{10}^2 >=< 0$, i.e., $\lambda_2^2 <=> \alpha_0(1+\chi^E)$. In Fig. 5, we considered $\lambda_2^2 = 9 \times 10^{11}$ dyne and in Fig. 7 we considered $\lambda_2^2 = 36 \times 10^{11}$ dyne. We observe from Figs. 5 and 7 that when $\lambda_2^2 < \alpha_0(1+\chi^E)$, V_1 has a cutoff frequency and V_2 exists for all values of frequency, while when $\lambda_2^2 > \alpha_0(1+\chi^E)$, V_2 has a cutoff frequency and V_1 exists for all values of frequency. This shows that the waves propagating with phase speeds V_1 and V_2 are strongly influenced by electric effect. In Fig. 6, the plot of V_1^2 and V_2^2 against the frequency ratio ω/ω_0 are shown when $c_6^2 - c_{10}^2 = 0$, we observe that the wave propagating with phase speed V_1 still faces cutoff frequency (as V_1^2 is negative in the range $0 < \omega/\omega_0 < 1.26$ and positive in the range $\omega/\omega_0 > 1.26$), while the wave propagating with phase speed V_2 exist for all positive values of frequency. In the Figs. 1, 3, 5, 6 and 7, the line which crosses the horizontal axis at critical frequency represents the vertical asymptote of the branches of the curve.

In Fig. 8, we have shown the curves of square of phase speeds V_1^2, V_2^2, V_3^2 and V_4^2, with respect to the frequency ratio, when $c_6^2 = c_{10}^2$. The waves propagating with phase speeds V_2 and V_4 are found to exist for all values of ω, while the waves propagating with phase speeds V_1 and V_3 propagate only if $\omega/\omega_0 > \sqrt{\frac{2\lambda_1}{3K}\left(\frac{j}{j_0}\right)}$ and $\omega/\omega_0 > \sqrt{2}$, respectively, otherwise they degenerate into distance decaying sinusoidal vibrations.

Next, we have computed the amplitude and energy ratios of various reflected waves when $c_6^2 - c_{10}^2 > 0$. In Fig. 9, we have plotted the modulus of reflection coefficients against the angle of incidence of coupled longitudinal wave propagating with phase speed V_1. We observe that the reflection coefficient Z_1 has maximum value equal to unity at normal incidence, it then decreases with increase of θ_0 till $\theta_0 = 68°$ and thereafter, it increases with increase in θ_0 and achieves its maximum value at grazing incidence. The reflection coefficient Z_2 begins with its maximum value at $\theta_0 = 0°$, then its value decreases with increase of angle of incidence. The modulus of reflection coefficients Z_3 and Z_4 increase with θ_0 till $\theta_0 = 42°$ and 46°, respectively, where they

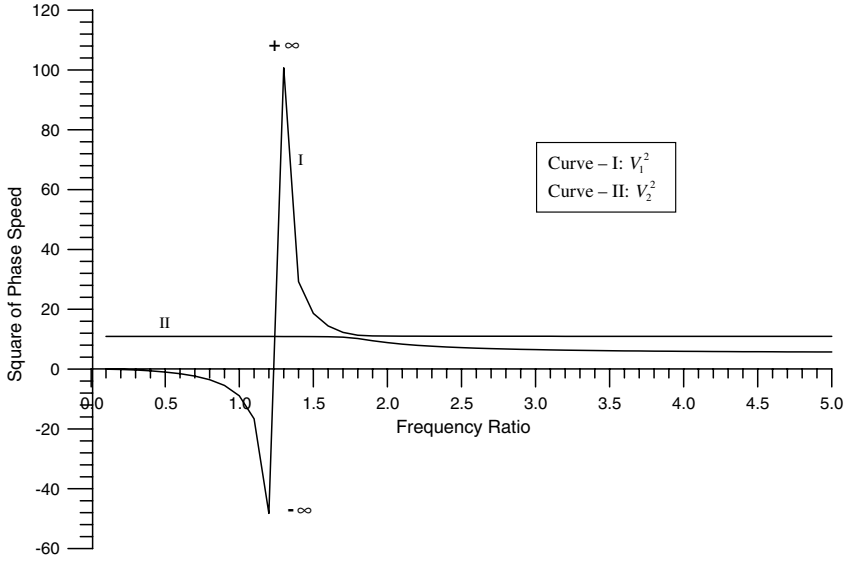

Fig. 5. Comparison of V_1^2 and V_2^2 at $\frac{\gamma}{\mu j} = 5.04$, when $\lambda_2^2 < \alpha_0(1+\chi^E)$.

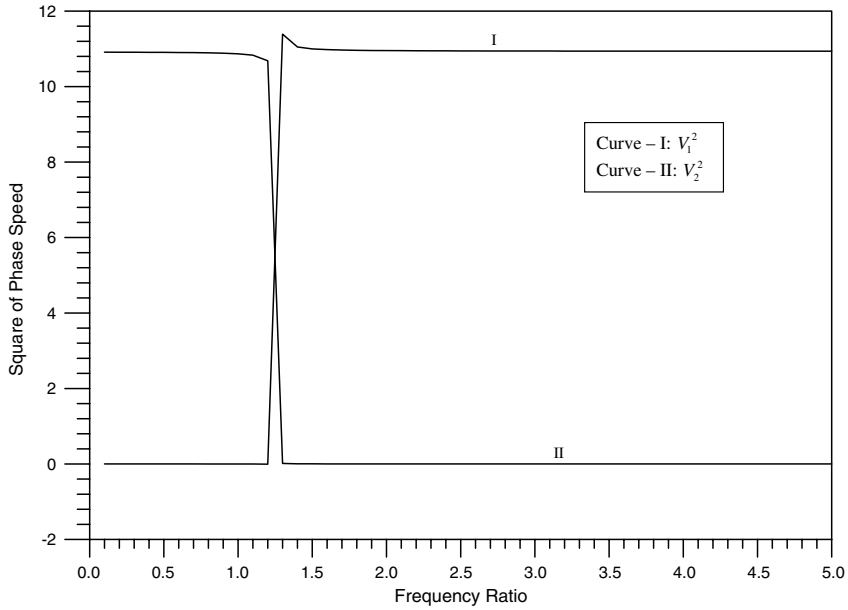

Fig. 6. Comparison of V_1^2 and V_2^2 at $\frac{\gamma}{\mu j} = 5.04$, when $\lambda_2^2 = \alpha_0(1 + \chi^E)$.

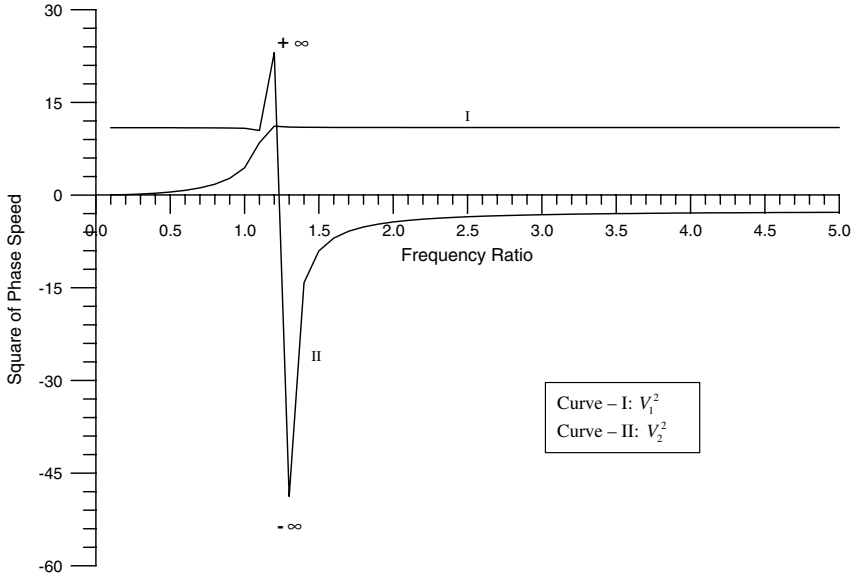

Fig. 7. Comparison of V_1^2 and V_2^2 at $\frac{\gamma}{\mu j} = 5.04$, when $\lambda_2^2 > \alpha_0(1 + \chi^E)$.

attain their maximum values. After this, their values decrease with increase in angle of incidence and approach to zero as θ_0 approaches 90°. The values of coefficients Z_2 and Z_3 are found to be very small as compared to the values of coefficients Z_1 and Z_4, so we have plotted each of them after magnifying 10^4 times their original values.

Fig. 10 depicts the variation of modulus of energy ratios of various reflected waves with the angle of incidence of coupled longitudinal wave propagating with speed V_1. It has been observed that the variation of each energy ratio of reflected waves is on the similar pattern as they were in their respective reflection coefficients.

Fig. 11 depicts the variation of modulus of reflection coefficients with the angle of incidence of coupled longitudinal wave propagating with speed V_2. Here, we have come across a critical angle at $\theta_0 = 39°$. We see that

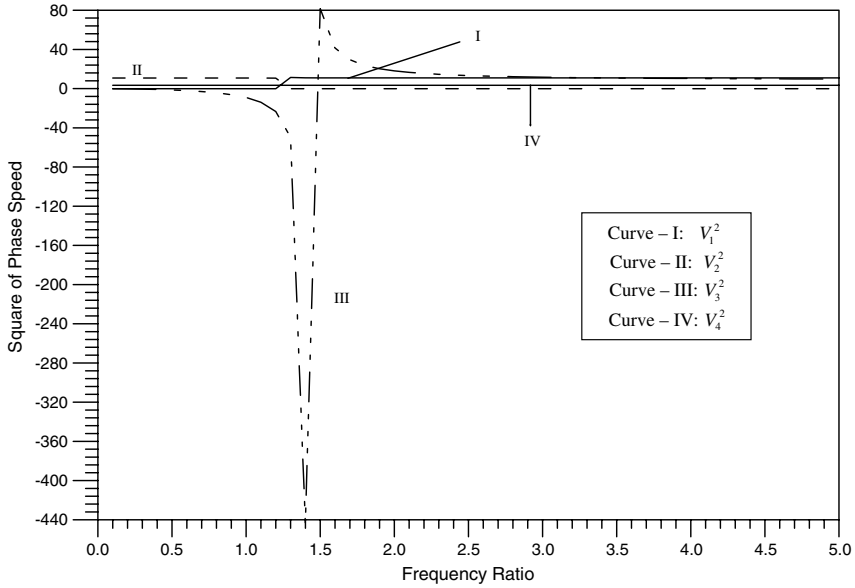

Fig. 8. Comparison of velocities when $\lambda_2^2 = \alpha_0(1 + \chi^E)$.

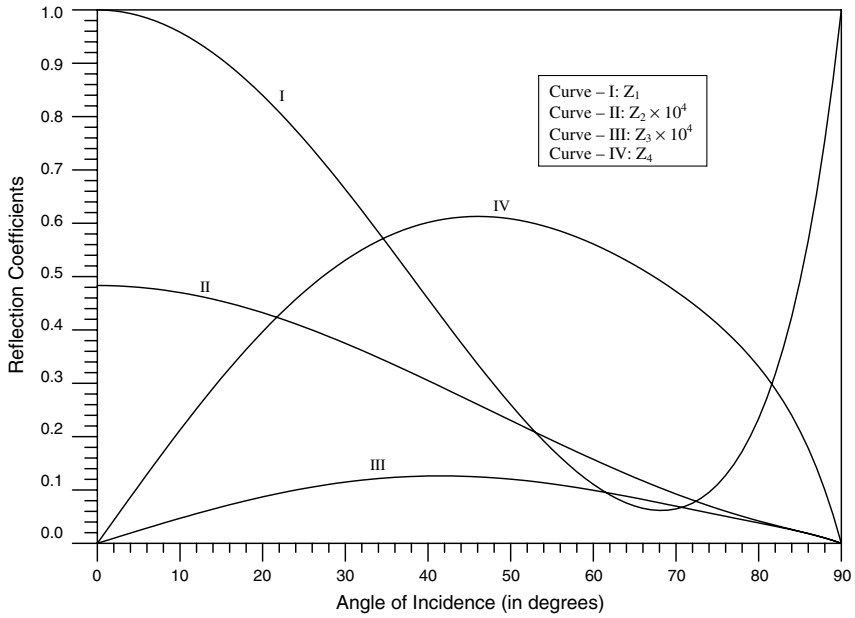

Fig. 9. Variation of modulus of reflection coefficients with angle of incidence of a set of coupled longitudinal waves with phase speed V_1.

at normal incidence, the reflection coefficient Z_1 has maximum value equal to 2.0, it then decreases with θ_0 till $\theta_0 = 31°$ and increases rapidly afterwards. The reflection coefficient Z_2 decreases slowly in the range $0° \leqslant \theta_0 < 39°$. The reflection coefficients Z_3 and Z_4 increase monotonically with increase in the angle of incidence.

Fig. 12 depicts the variation of modulus of energy ratios of the reflected waves with the angle of incidence of coupled longitudinal wave propagating with the speed V_2. It is seen that the waves propagating with phase speeds V_1 and V_4 carry very small amount of energy in comparison to the amount of energy carried by the

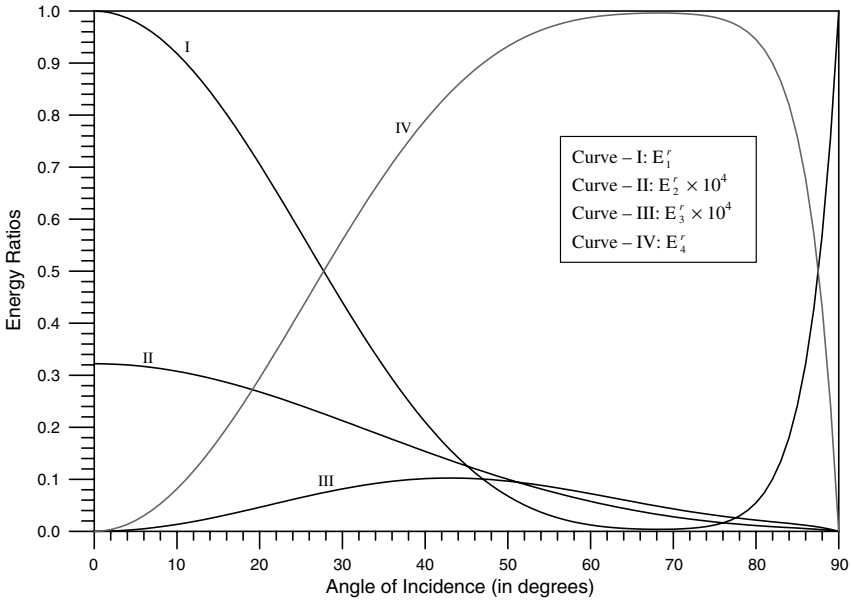

Fig. 10. Variation of modulus of energy ratios versus angle of incidence of a set of coupled longitudinal wave with phase speed V_1.

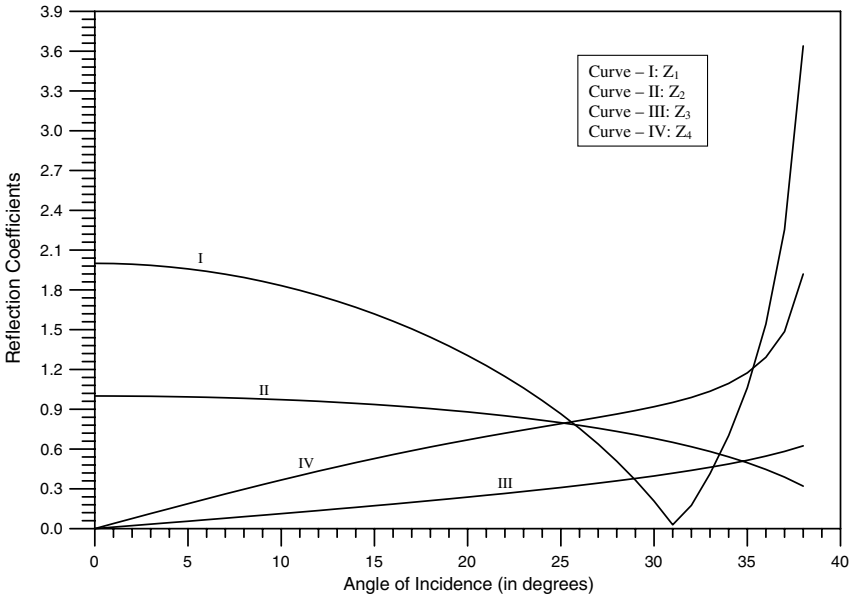

Fig. 11. Variation of modulus of reflection coefficients with angle of incidence of a set of coupled longitudinal waves with phase speed V_2.

reflected wave propagating with phase speed V_2. We have plotted the curves of E_1^r and E_4^r after magnifying their original values with the factor 10^3.

In Fig. 13, we have shown the variation of modulus of reflection coefficients versus angle of incidence of coupled transverse wave with speed V_3. We found that $\theta_0 = 67°$ acts as a critical angle. The reflection coefficients Z_1 and Z_2 begin with the value zero at the normal incidence, thereafter, both Z_1 and Z_2 increase rapidly with increase in θ_0, but at different rates. The reflection coefficient Z_2 also increases with increase in the angle of incidence, but with the rate less than that of Z_1 and Z_2. The reflection coefficient Z_3 starts decreasing from

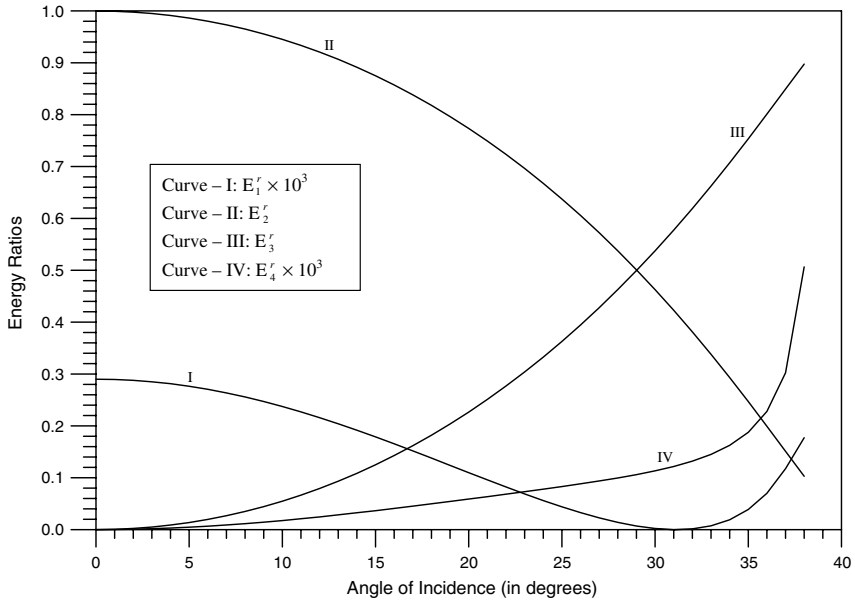

Fig. 12. Variation of modulus of energy ratios versus angle of incidence of a set of coupled longitudinal wave with phase speed V_2.

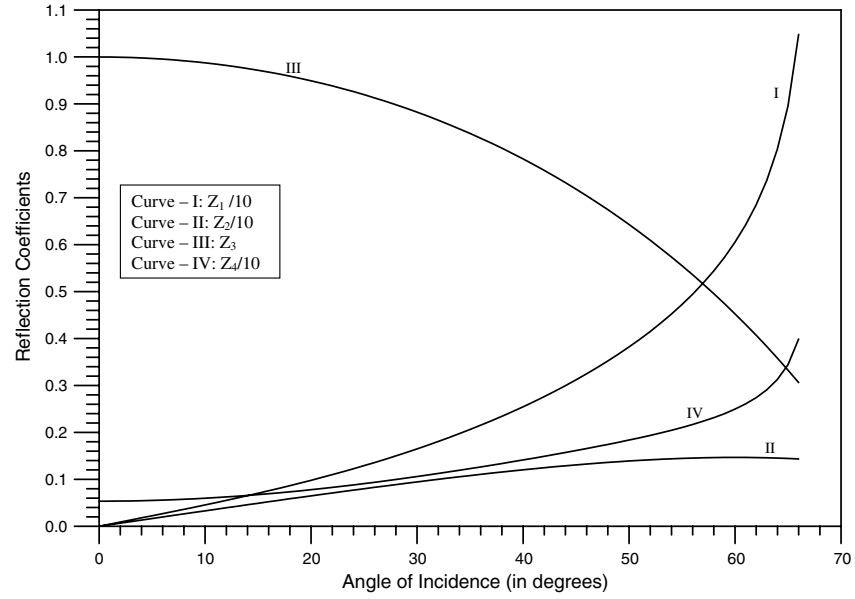

Fig. 13. Variation of modulus of reflection coefficients with angle of incidence of a set of coupled transverse waves with phase speed V_3.

the value 1 with the angle of incidence θ_0 in the range $0° \leqslant \theta_0 < 67°$. We have plotted the reflection coefficients Z_1, Z_2 and Z_4 by dividing their original values with 10.

Fig. 14 depicts the variation of modulus of energy ratios of the reflected waves against the angle of incidence of coupled transverse wave propagating with speed V_3. It is seen that the energy ratios corresponding to the waves with speeds V_1 and V_4 are so small as compared to the energy ratio corresponding to the wave traveling with speed V_3 that we have plotted each of them by magnifying their original values with the factor 10^3.

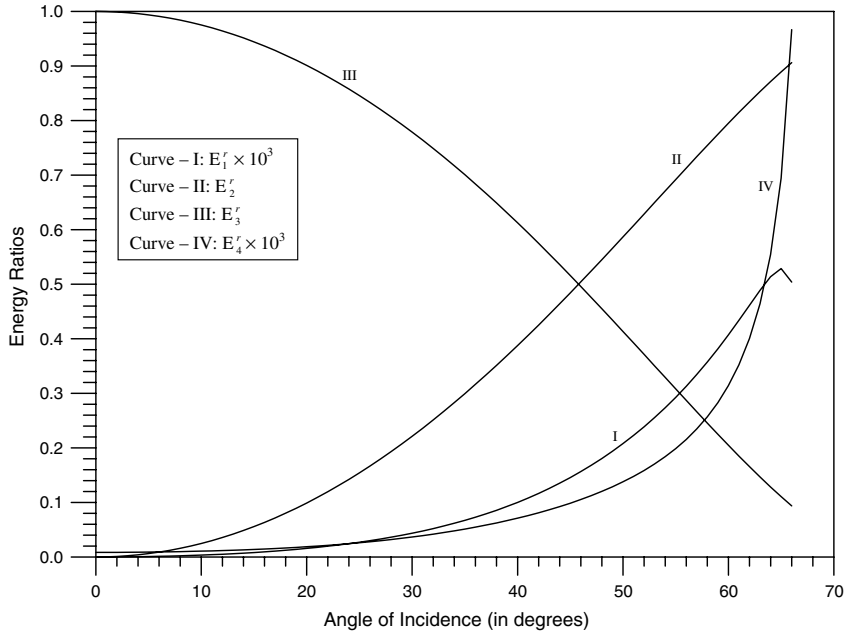

Fig. 14. Variation of modulus of energy ratios versus angle of incidence of a set of coupled transverse wave with speed V_3.

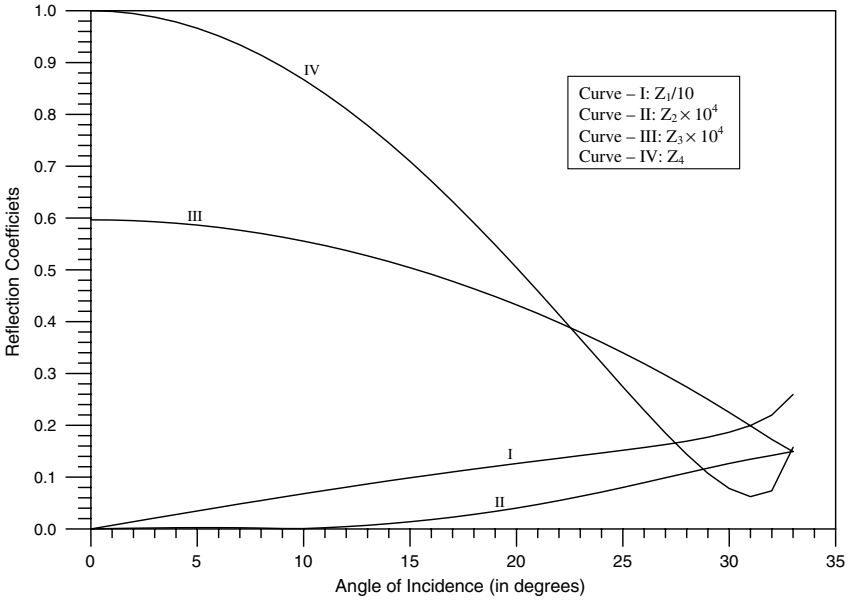

Fig. 15. Variation of modulus of reflection coefficients with angle of incidence of a set of coupled transverse waves with phase speed V_4.

In Fig. 15, we have plotted the modulus of reflection coefficients as a function of the angle of incidence of coupled transverse wave propagating with speed V_4. Here, we obtained a critical angle at $\theta_0 = 34°$. The modulus of reflection coefficients Z_1 and Z_2 have zero value at normal incidence. Their values increase with increase in the angle of incidence and attain their maximum values at $\theta_0 = 33°$. The reflection coefficient Z_3 begins with its maximum value at normal incidence and decreases in the range $0° \leqslant \theta_0 \leqslant 34°$. The value of reflection coefficient Z_4 is found maximum at $\theta_0 = 0°$ and it decreases in the range $0° \leqslant \theta_0 \leqslant 31°$. Afterwards,

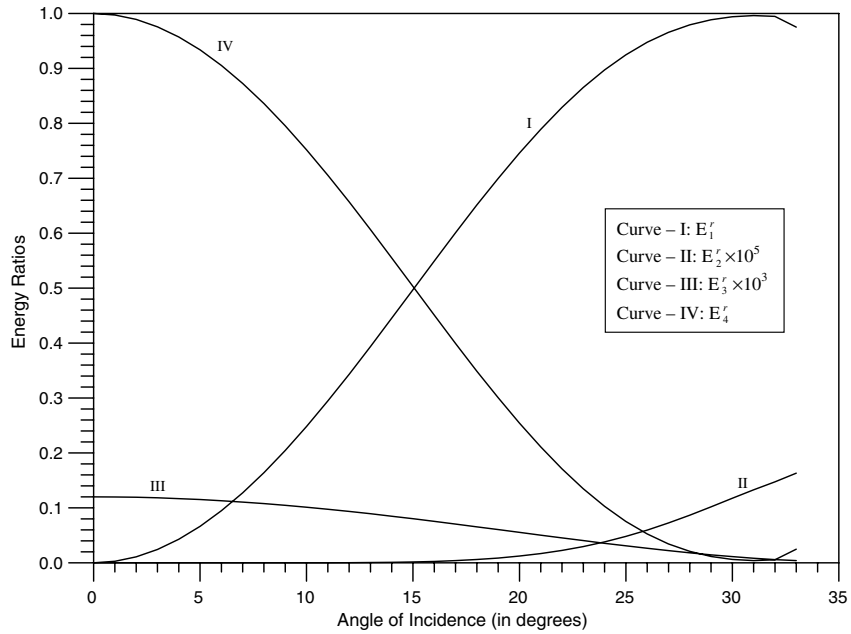

Fig. 16. Variation of modulus of energy ratios versus angle of incidence of a set of coupled transverse wave with speed V_4.

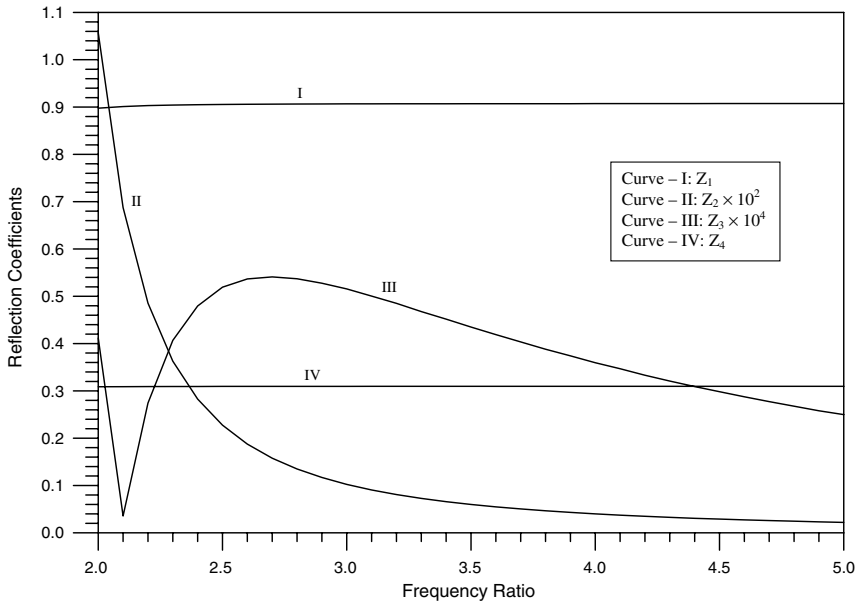

Fig. 17. Variation of modulus of reflection coefficients with frequency ratio (ω/ω_0) when a set of coupled longitudinal waves with phase speed V_1 is incident at an angle $\theta_0 = 15°$.

it increases with increase in θ_0, but to a very small extent. We have plotted the variation of coefficients Z_1, Z_2 and Z_3 by magnifying their original values with the factors 10^{-1}, 10^4 and 10^4, respectively.

In Fig. 16, we have plotted the variation of modulus of energy ratios with the angle of incidence of coupled transverse wave traveling with speed V_4. We have plotted the energy ratios E_2^r and E_3^r by multiplying their original values with factors 10^5 and 10^3, respectively.

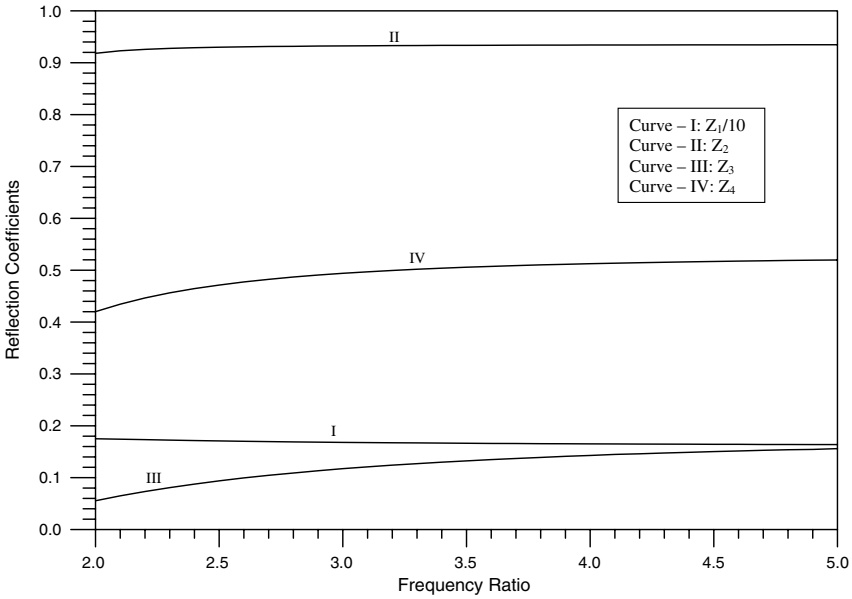

Fig. 18. Variation of modulus of reflection coefficients with frequency ratio (ω/ω_0) when a set of coupled longitudinal waves with phase speed V_2 is incident at an angle $\theta_0 = 15°$.

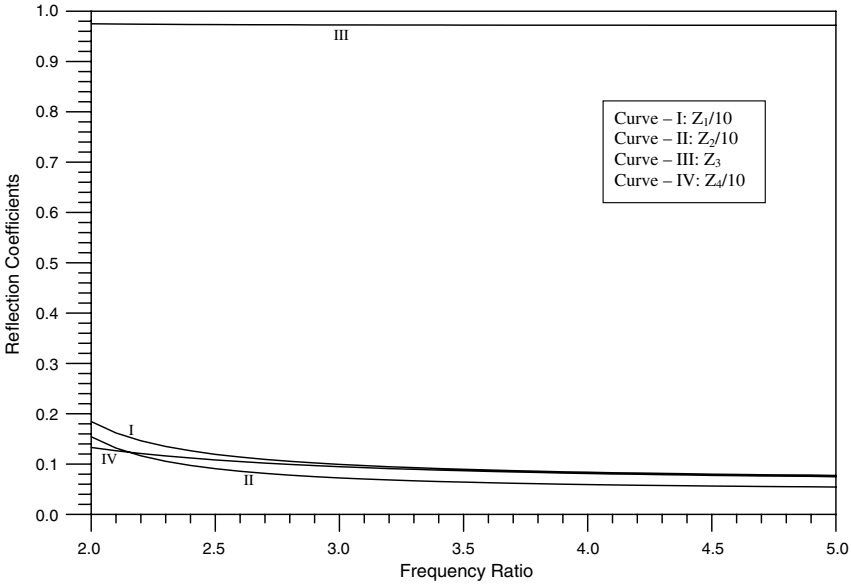

Fig. 19. Variation of modulus of reflection coefficients with frequency ratio (ω/ω_0) when a set of coupled transverse waves with phase speed V_3 is incident at an angle $\theta_0 = 15°$.

In Figs. 10, 12, 14 and 16, it has been verified that the sum of energy ratios of various reflected waves is equal to unity at each angle of incidence, showing that their is no dissipation of energy at the free plane boundary surface of $\mathfrak{R}$ during reflection.

Figs. 17–20 depict the variation of modulus of reflection coefficients with the frequency ratio $\omega/\omega_0 \geqslant 2$ when each of the coupled wave is made incident at an angle of incidence $\theta_0 = 15°$ at the free surface. It is worth

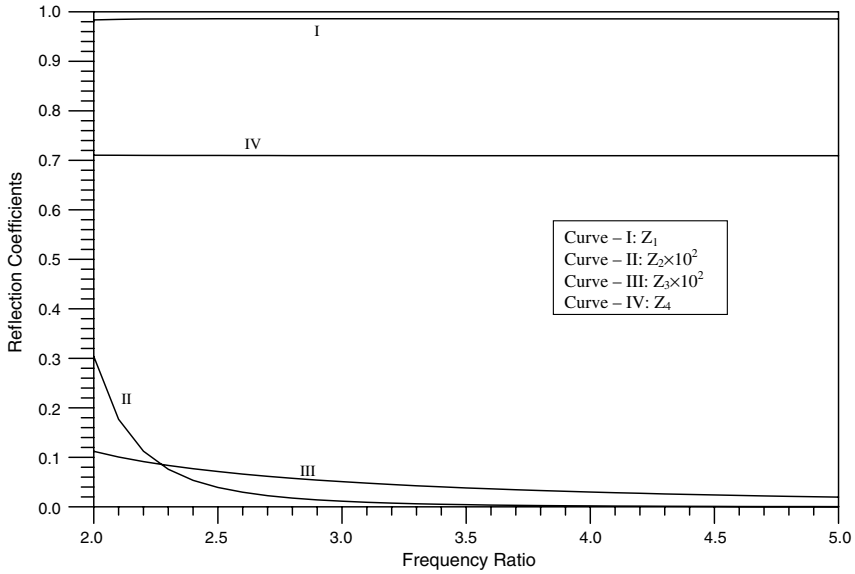

Fig. 20. Variation of modulus of reflection coefficients with frequency ratio (ω/ω_0) when a set of coupled transverse waves with phase speed V_4 is incident at an angle $\theta_0 = 15°$.

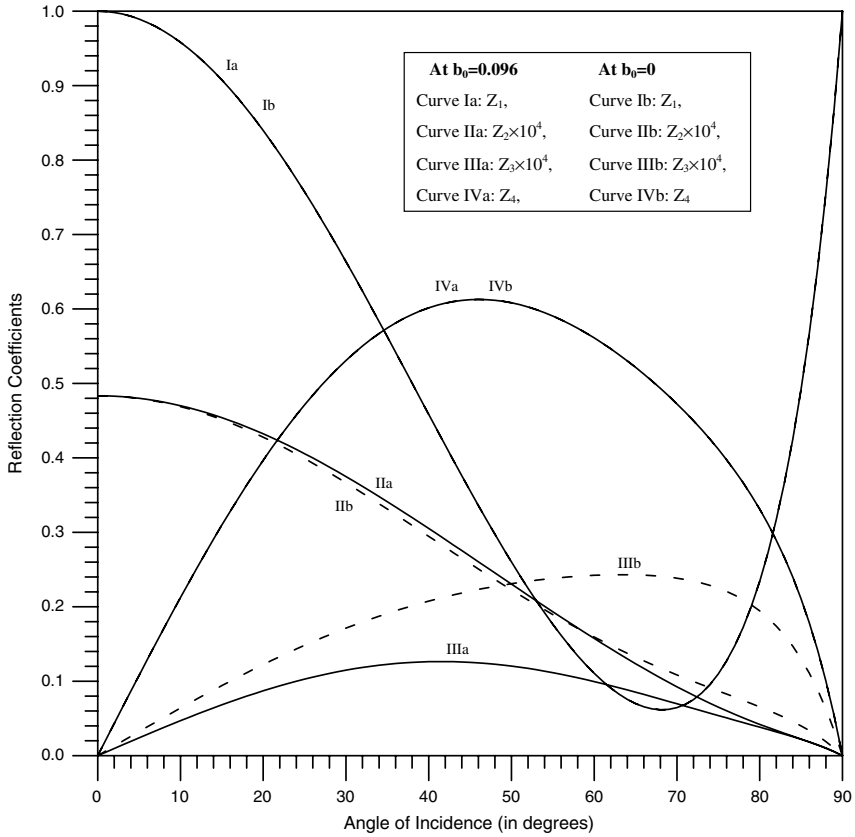

Fig. 21. Effect of constant b_0 on modulus of reflection coefficients when a set of coupled longitudinal waves with phase speed V_1 is incident.

to mention here that the amplitude ratio of those reflected waves propagating with the speed as that of the incident wave are least affected by the frequency parameter.

In Fig. 17, we have shown the variation of reflection coefficients when a coupled longitudinal wave with speed V_1 is made incident. We have plotted Z_2 and Z_3 by magnifying their original values with the factors 10^2 and 10^4, respectively. It is found that the amplitude ratios Z_1, Z_2 and Z_4 are almost constant for higher values of frequency ratio.

Fig. 18 depicts the variation of reflection coefficients for an incident coupled longitudinal wave with speed V_2. The value of coefficient Z_1 is greater than the other coefficients at each value of frequency ratio. The reflection coefficients Z_1 and Z_2 remain almost constant in the entire range. The other coefficients begin with their minimum values and then they increase very slowly. We have plotted the coefficient Z_1 by dividing its original value with 10.

Fig. 19 depicts the variation of reflection coefficients when a coupled transverse wave with speed V_3 is made incident. We notice from this figure that the amplitude ratios Z_1 and Z_2 behave alike with the frequency ratio, while Z_3 is almost independent of frequency ratio. We have plotted the reflection coefficients Z_1, Z_2 and Z_4 by dividing their original values with 10.

Fig. 20 depicts the variation of reflection coefficients for an incident coupled transverse wave traveling with speed V_4. Here, the reflection coefficients Z_1 and Z_4 are almost independent of the frequency ratio. However, the reflection coefficients Z_2 and Z_3 decrease with increase in the frequency ratio. The values of coefficients Z_2 and Z_3 are very small and their curves are shown by multiplying their original values with the factor 10^2.

In Figs. 21–24, we have shown the effect of micro-stretch parameter b_0 on the reflection coefficients plotted against the angle of incidence of each set of coupled waves (that is, coupled longitudinal waves and coupled

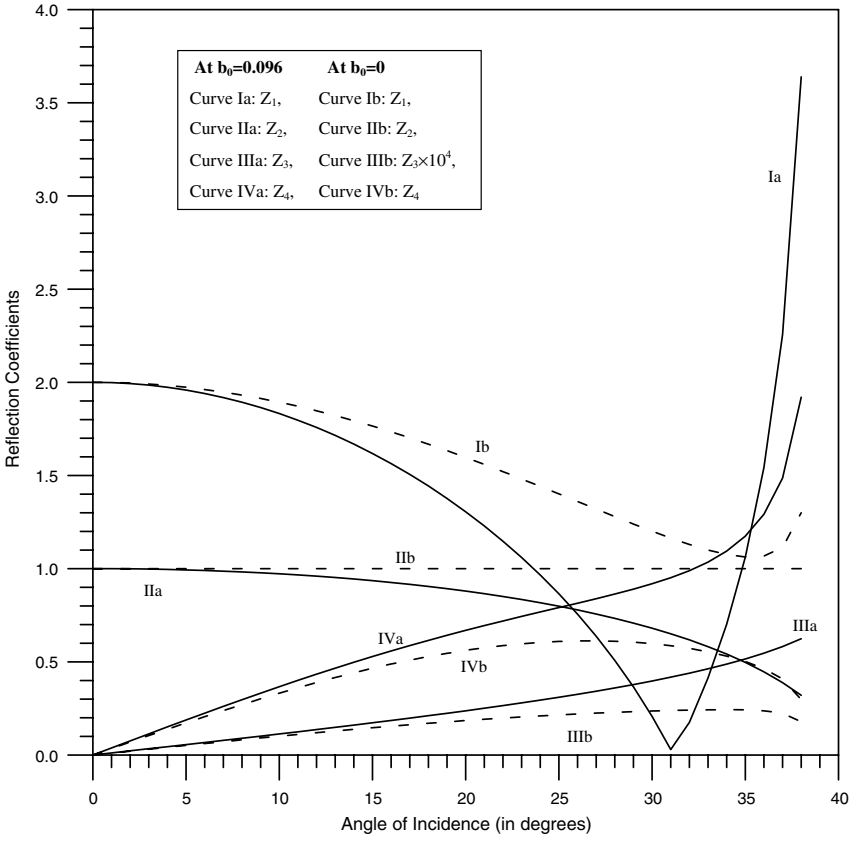

Fig. 22. Effect of constant b_0 on modulus of reflection coefficients when a set of coupled longitudinal waves with phase speed V_2 is incident.

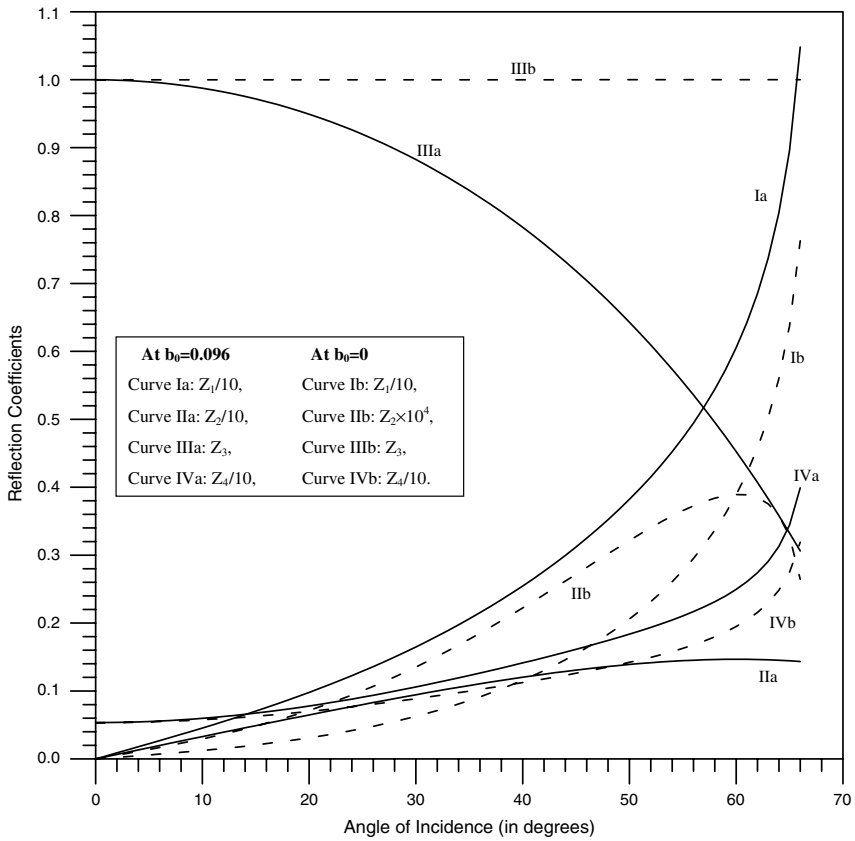

Fig. 23. Effect of constant b_0 on modulus of reflection coefficients when a set of coupled transverse waves with phase speed V_3 is incident.

transverse waves). It is clear from these figures that the reflection coefficients are significantly influenced by the parameter b_0.

7. Conclusions and remarks

In this paper, we have obtained the condition on propagation of each plane wave in an infinite electro-microelastic solid and investigated the reflection phenomenon of each set of coupled waves striking separately at a stress free plane boundary of an electro-microelastic solid half-space. It can be seen that the longitudinal microrotational wave propagating with phase speed V_5 is not influenced by the electro-microelastic effect and behaves in a same way as in micropolar elasticity. Therefore, its reflection phenomenon from the plane stress free boundary of an electro-microelastic half-space will be the same as investigated earlier by Parfitt and Eringen (1969). This is the reason, we have not considered the reflection problem corresponding to incident longitudinal microrotational wave propagating with phase speed V_5. We conclude that

(1) Three waves are found to disappear below a critical frequency depending upon the properties of the medium. These waves are (i) a set of coupled longitudinal waves propagating with phase speed V_1 when $c_6^2 - c_{10}^2 \geqslant 0$, otherwise the set of coupled longitudinal waves propagating with phase speed V_2, (ii) a set of coupled transverse waves propagating with phase speed V_3 and (iii) a longitudinal microrotational wave traveling independently with phase speed V_5. The value of cutoff frequency for the coupled longitudinal waves is found to be different from that of for the coupled transverse waves and for the longitudinal microrotational wave.

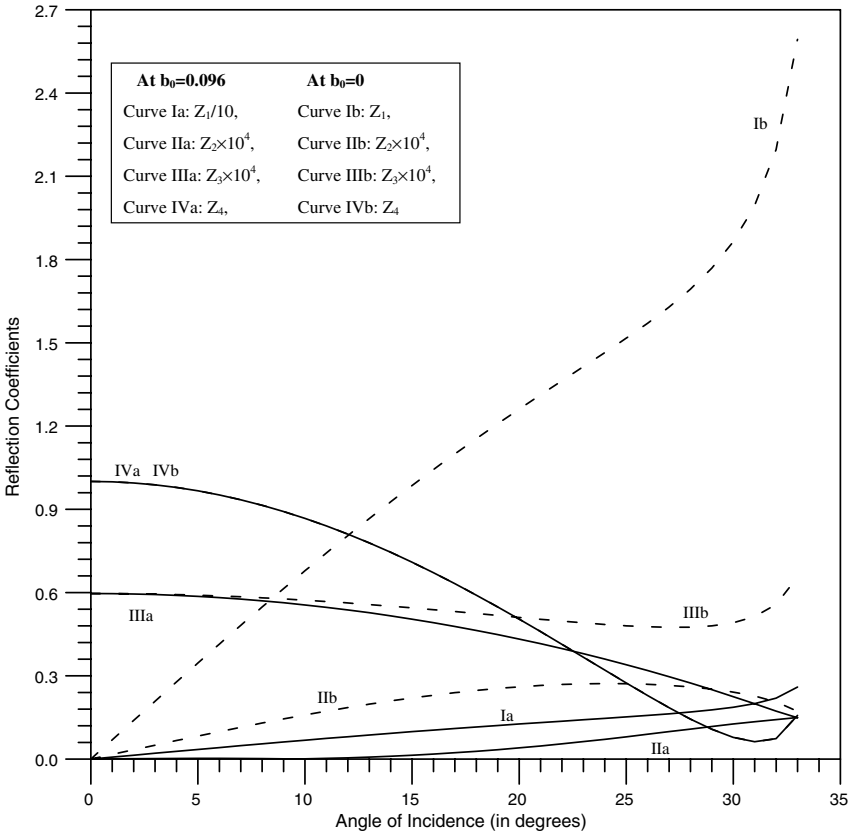

Fig. 24. Effect of constant b_0 on modulus of reflection coefficients when a set of coupled transverse waves with phase speed V_4 is incident.

(2) An additional inequality $\frac{2}{j_0}\left(\alpha_0 - \frac{\lambda_2^2}{1+\chi^E}\right) \leqslant \lambda + 2\mu + K$ must be satisfied for the consistent solution of V_1^2 and V_2^2.
(3) In case of an oblique incidence of elastic waves at free plane boundary of an electro-microelastic soild half-space, the reflection coefficients are found to be the functions of the angle of incidence, frequency and elastic properties of the medium.
(4) The sum of energy ratios at each angle of incidence of any set of coupled longitudinal waves and coupled transverse waves is found to be unity. This shows that there is no dissipation of energy at the stress free plane boundary surface during reflection.

Acknowledgements

Authors are thankful to Council of Scientific and Industrial Research, New Delhi for providing financial assistance in the form of SRF to AK and through Grant No. 25 (0134)/04/EMR-II to S.K.T for completing this study. Authors are also grateful to the unknown reviewers for examining the manuscript critically and suggesting various improvements.

References

Achenbach, J.D., 1973. Wave Propagation in Elastic Solids. North Holland, Amsterdam.
Ariman, T., 1972. Wave propagation in a micropolar elastic half-space. Acta Mech. 13, 11–20.
Eringen, A.C., Suhubi, E.S., 1964a. Nonlinear theory of simple microelastic solids I. Int. J. Engng. Sci. 2, 189–203.
Eringen, A.C., 1966. Linear theory of micropolar elasticity. J. Math. Mech. 15, 909–923.

Smith, A.C., 1967. Waves in micropolar elastic solids. Int. J. Engng. Sci. 5, 741–746.
Eringen, A.C., 2004. Electromagnetic theory of microstretch elasticity and bone modeling. Int. J. Engng. Sci. 42, 231–242.
Eringen, A.C., 1999. Microcontinuum Field Theories I: Foundations and Solids. Springer-Verlag, New York.
Eringen, A.C., Maugin, G.A., 1990. Electrodynamics of Continua I Foundations and Solid Media. Springer-Verlag, New York.
Eringen, A.C., 1990. Theory of thermo-microstretch elastic solids. Int. J. Engng. Sci. 28, 1291–1301.
Khurana, A., Tomar, S.K., 2007. Propagation of plane elastic waves at a plane interface between two electro-microelastic solid half-spaces. Int. J. Solids Struct. 44, 3773–3795.
Nowacki, W., Nowacki, W.K., 1969. Generation of waves in infinite micropolar elastic solid body I, II. Bull. Acad. Pol. Sci. Tech. 17, 39–47 (49–56).
Parfitt, V.R., Eringen, A.C., 1969. Reflection of plane waves from a flat boundary of a micropolar elastic half-space. J. Acoust. Soc. Am. 45, 1258–1272.
Suhubi, E.S., Eringen, A.C., 1964b. Nonlinear theory of simple microelastic solids II. Int. J. Engng. Sci. 2, 389–404.
Tomar, S.K., Gogna, M.L., 1995. Reflection and refraction of coupled transverse and microrotational waves at an interface between two micropolar elastic media in welded contact. Int. J. Engng. Sci. 33, 485–496.
Tomar, S.K., Gogna, M.L., 1995. Reflection and refraction of longitudinal waves at an interface between two micropolar elastic media in welded contact. J. Acoust. Soc. Am. 97, 822–830, Erratum: in J. Acoust. Soc. Am. 102, (1997), 2452.
Tomar, S.K., Kumar, R., Kaushik, V.P., 1998. Wave propagation in a micropolar elastic medium with stretch. Int. J. Engng. Sci. 36, 683–698.
Tomar, S.K., Garg, M., 2005. Reflection and transmission of waves from a plane interface between two microstretch solid half-spaces. Int. J. Engng. Sci. 43, 139–169, Errata in Int. J. Engng. Sci. 44, (2006), 285–287.